NSF/MUSES, grant no OAC-2103680.

Illinois Center for Advanced Studies of the Universe

Location of the Critical Point from Holography

e-Print: 2309.00579 [nucl-th]

Jorge Noronha

SUNDAY DISCUSSION

M. Hippert, J. Grefa, I. Portillo, J. Noronha-Hostler, C. Ratti, R. Rougemont and M. Trujillo

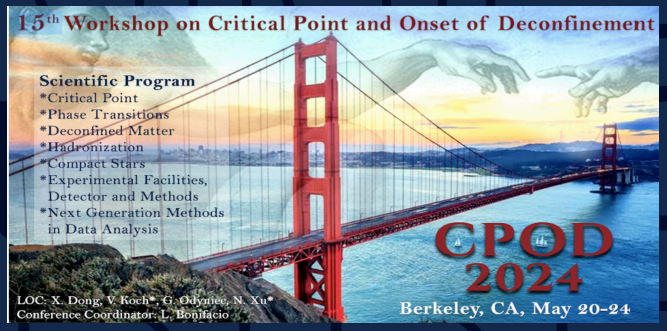

Holography + Lattice results at $\mu = 0$

Bayesian inference

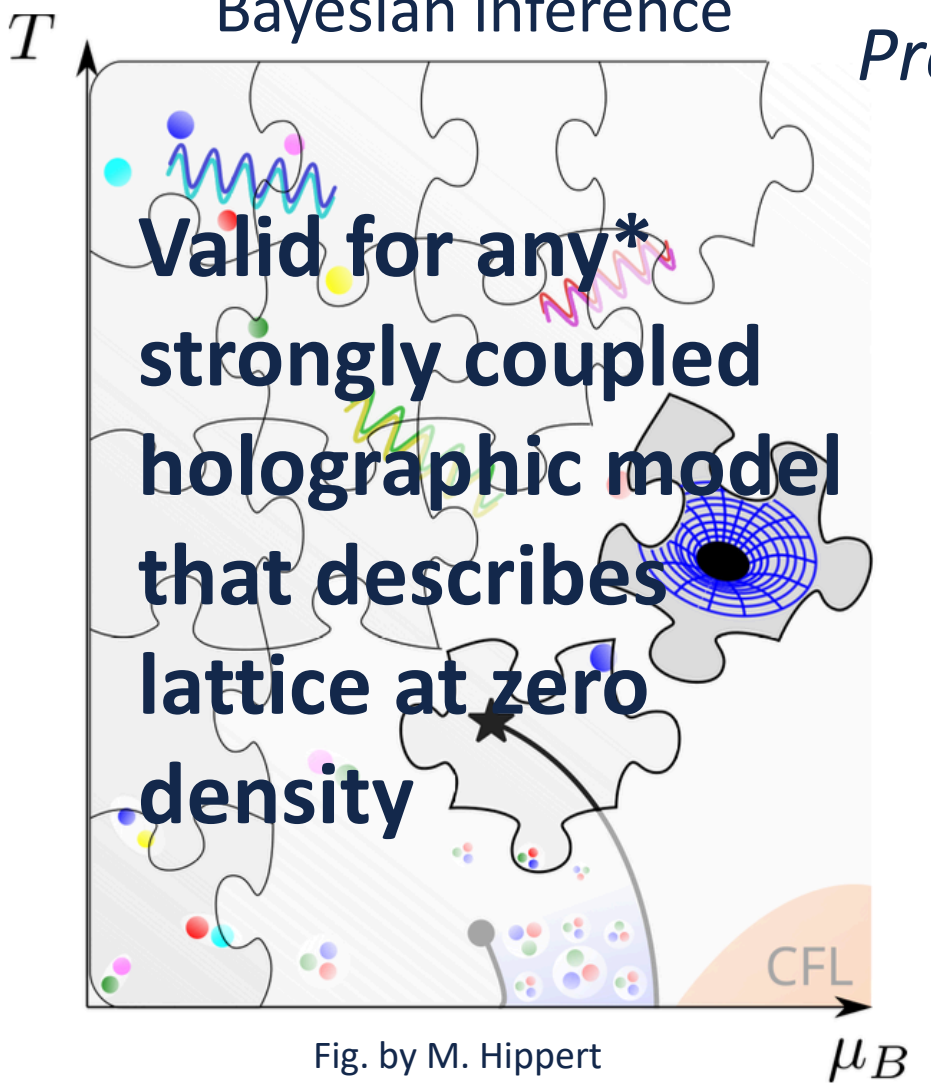

Fig. by M. Hippert

Predict CEP (95% confidence level):

$$T_c = 101 - 108 \text{ MeV}$$

$$\mu_c = 560 - 625 \text{ MeV}$$

$$\sqrt{s} = 4.0 \; - \; 4.8 \text{ GeV}$$

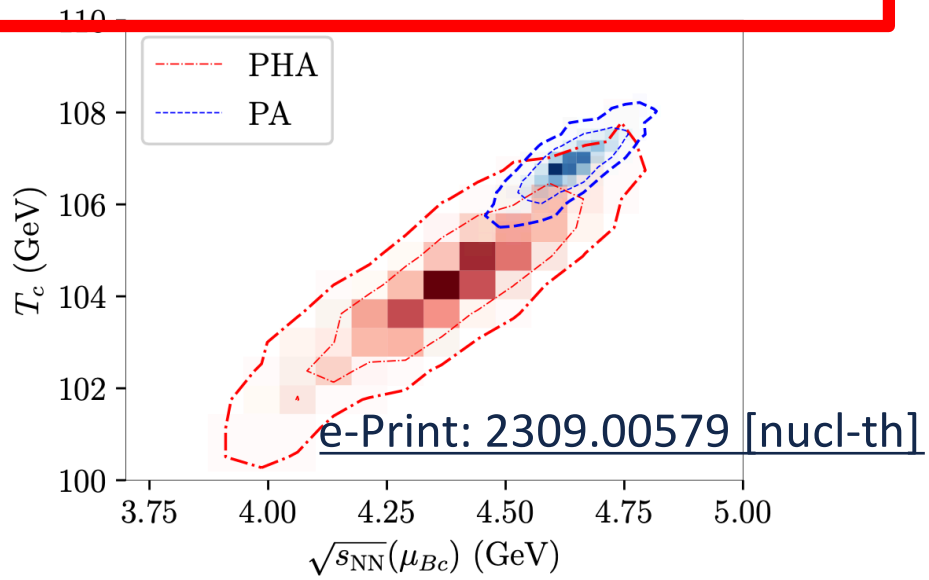

e-Print: 2309.00579 [nucl-th]

Nearly perfect fluidity

An emergent property of QCD

J. Noronha-Hostler, JN, C. Greiner
PRL (2009)

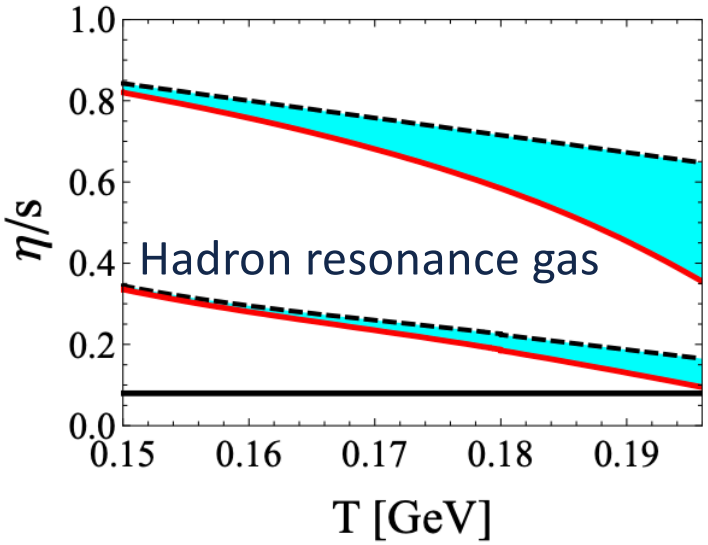

Low temperatures
(hadron resonance gas)

Kovtun, Son, Starinets,
PRL (2005)

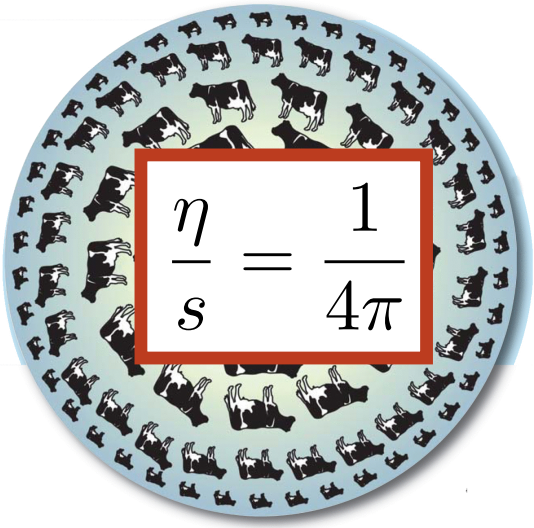

AdS/CFT duality

Arnold, Moore, Yaffe
(2000), (2003)

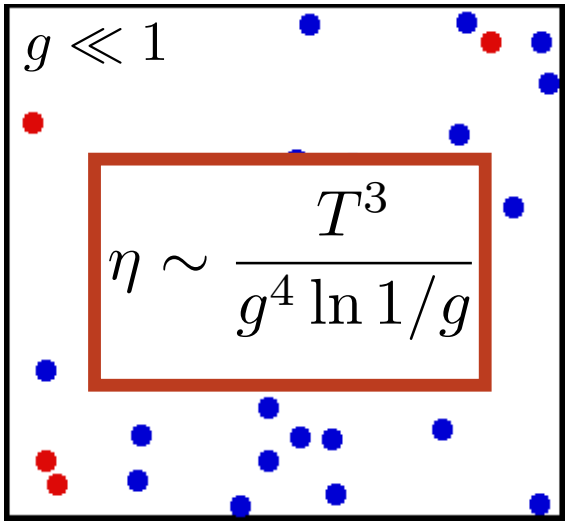

High temperatures
(quasiquarks, quasigluons)

Nearly perfect fluidity of the QGP

An emergent property of QCD

Holographic duality

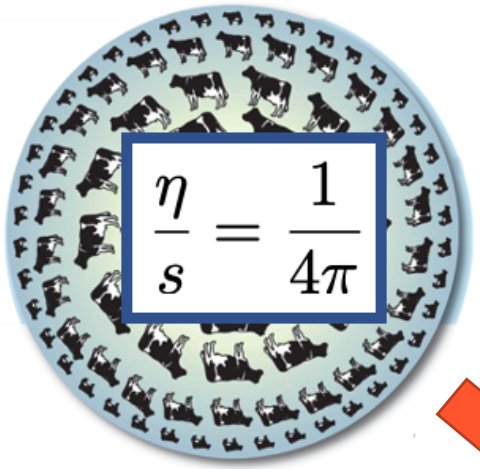

Kovtun, Son, Starinets, PRL (2005)

Bernhard, Moreland, Bass, Nature Physics, (2019)

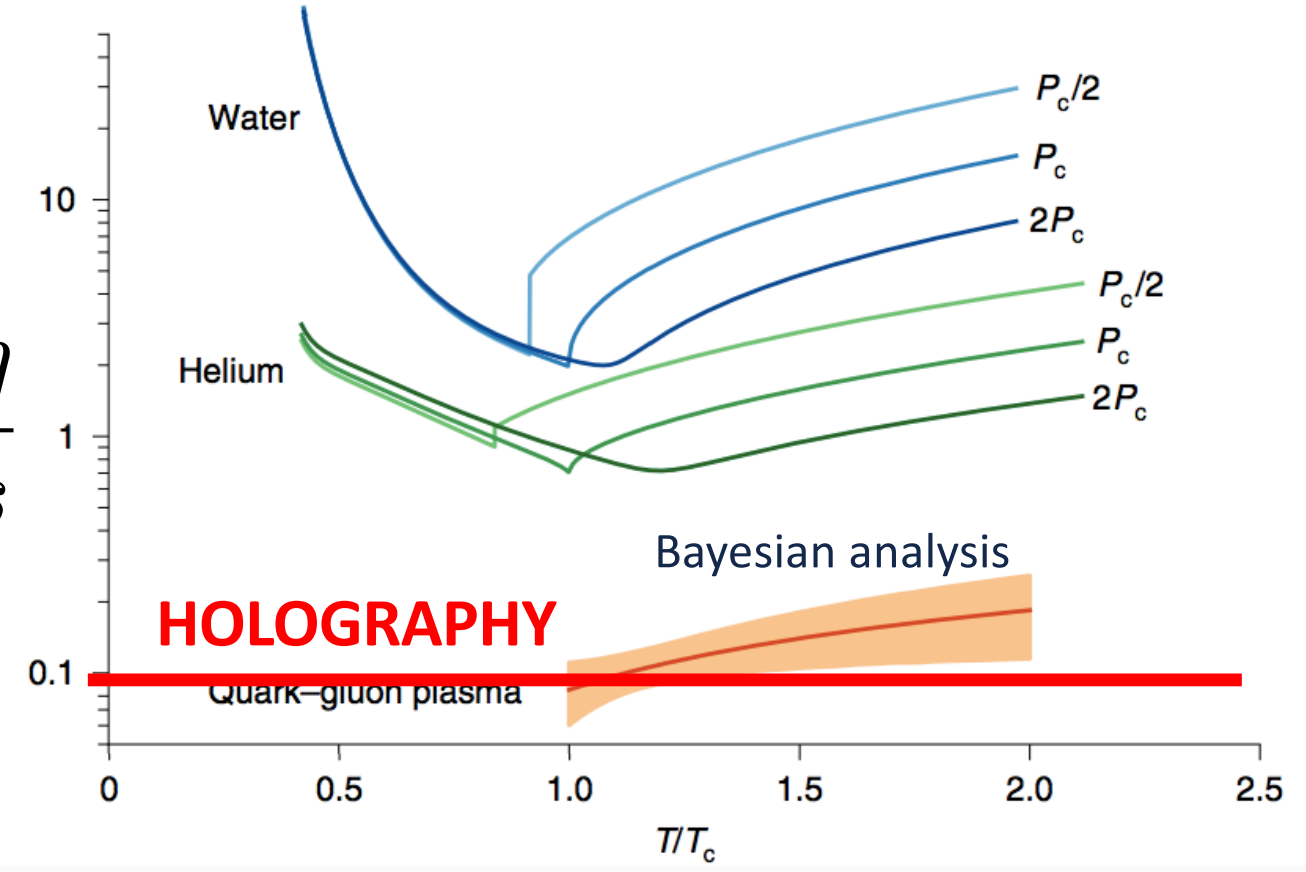

What is the holographic duality?

Maldacena, 1997; Witten, 1998, Gubser, Polyakov, Klebanov, 1998

"Strongly coupled plasmas from black hole physics"

Strongly coupled
non-Abelian plasma

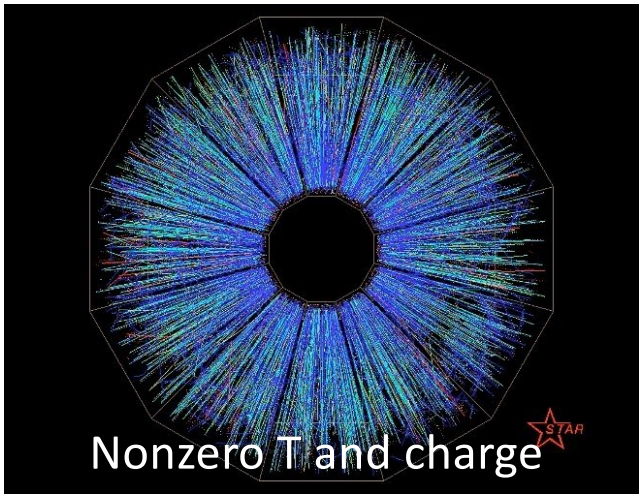

DUALITY

≈

Classical gravity in d>4

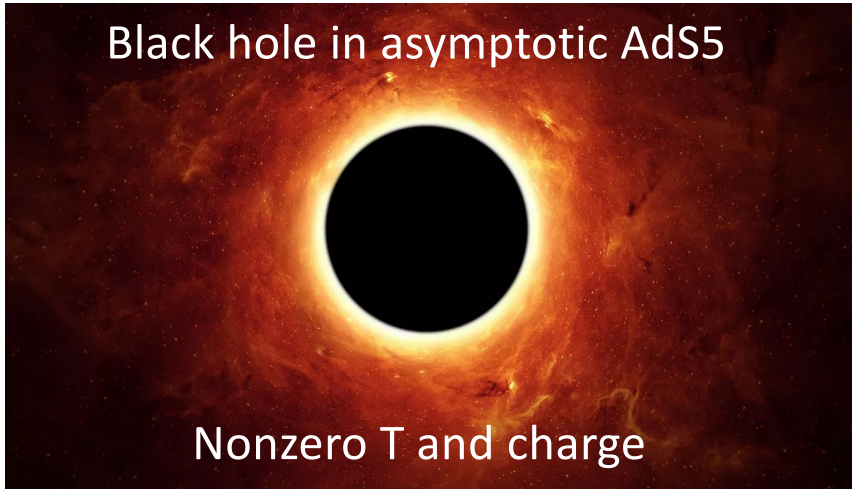

How is this used to find the QCD CP?

Black hole

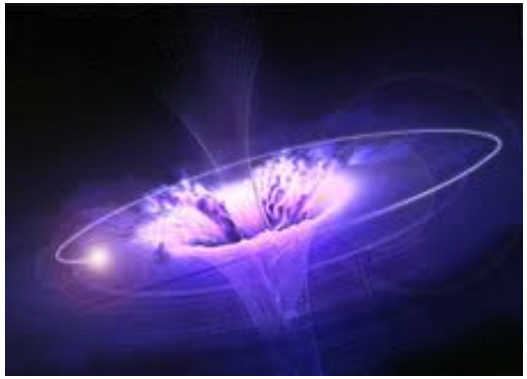

+

Anti-de Sitter (AdS) space

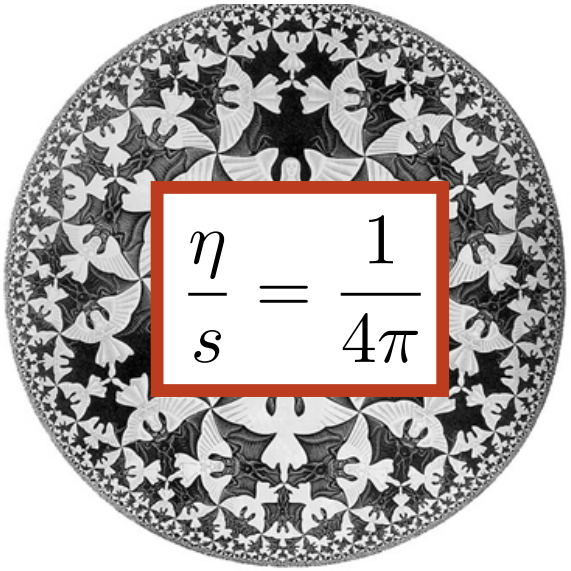

=

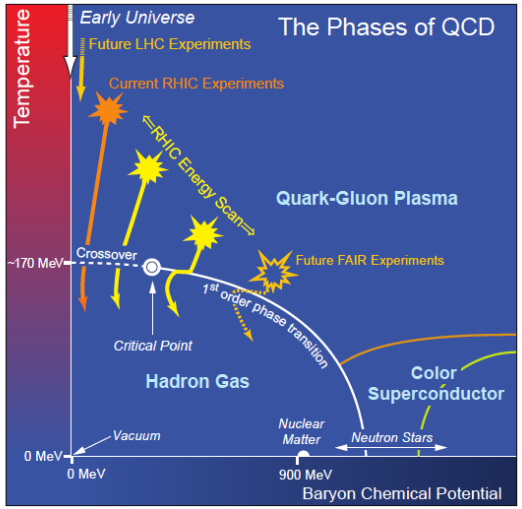

Nearly perfect fluidity

Black Hole "Engineering"

DeWolfe, Gubser, Rosen, PRD (2011)
Finazzo et al, JHEP (2015)
Rougemont et al. PRL (2015), JHEP (2016),PRD (2017)
Critelli et al, PRD (2017)
Grefa et al, PRD (2021), PRD (2022)
Hippert et al., 2309.00579 [nucl-th]

Black hole engineering in AdS

- Black hole solutions of Einstein-Maxwell-Dilaton equations

See the review by Rougemont et al, Progress in Particle and Nuclear Physics 135 (2024)

$$S = \frac{1}{2\kappa_5^2}\int_{\mathcal{M}_5} d^5x\sqrt{-g}\left[R - \frac{(\partial_\mu\phi)^2}{2} - V(\phi) - \frac{f(\phi)F_{\mu\nu}^2}{4}\right]$$

Dilaton field dual to $\langle \mathrm{Tr}F^2\rangle$

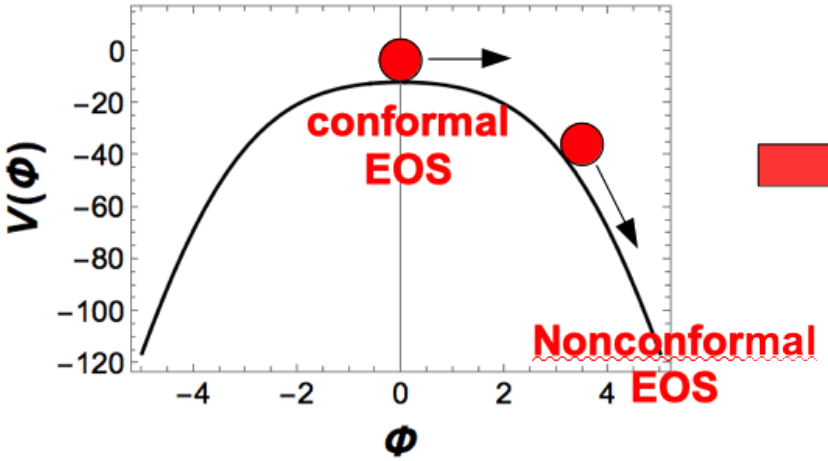

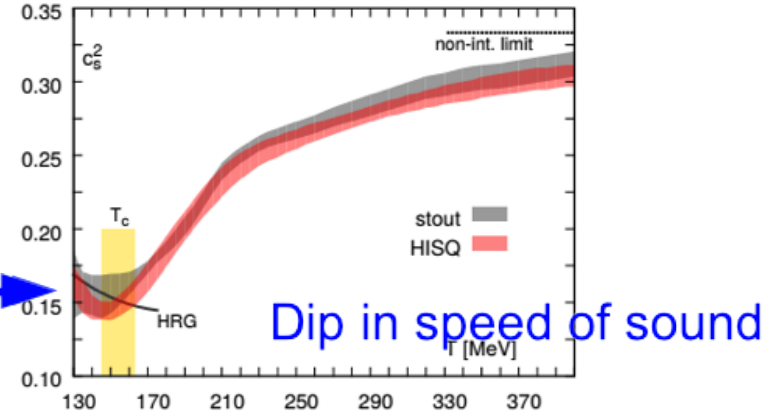

Black hole engineering in AdS

- Black hole solutions of Einstein-Maxwell-Dilaton equations

See the review by Rougemont et al, Progress in Particle and Nuclear Physics 135 (2024)

$$S = \frac{1}{2\kappa_5^2}\int_{\mathcal{M}_5} d^5x\sqrt{-g}\left[R - \frac{(\partial_\mu\phi)^2}{2} - V(\phi) - \frac{f(\phi)F_{\mu\nu}^2}{4}\right]$$

Dilaton field dual to $\langle \mathrm{Tr}F^2\rangle$

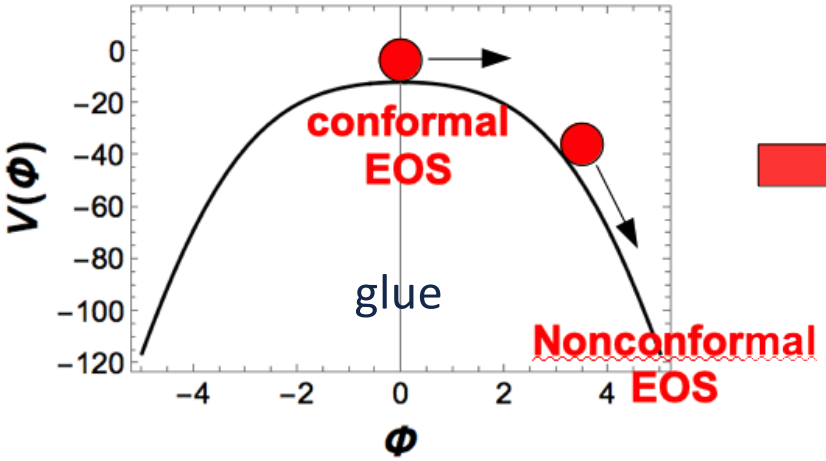

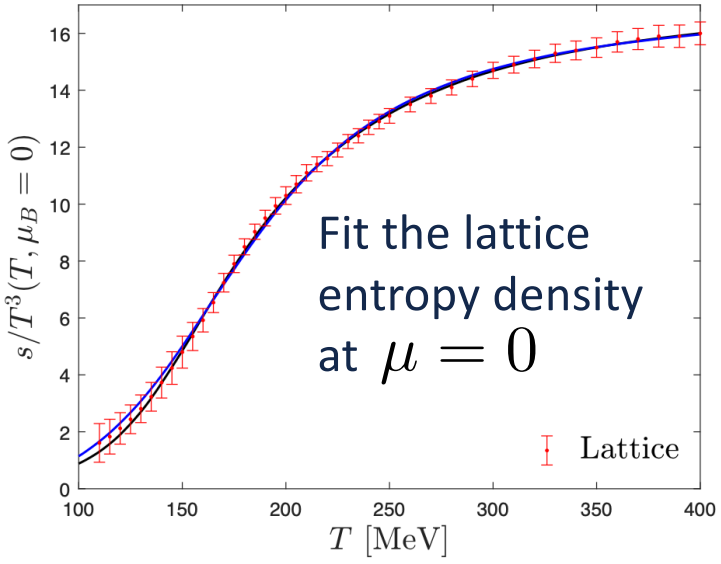

Black hole engineering in AdS

- Black hole solutions of Einstein-Maxwell-Dilaton equations

See the review by Rougemont et al, Progress in Particle and Nuclear Physics 135 (2024)

$$S = \frac{1}{2\kappa_5^2}\int_{\mathcal{M}_5} d^5x\sqrt{-g}\left[R - \frac{(\partial_\mu\phi)^2}{2} - V(\phi) - \frac{f(\phi)F_{\mu\nu}^2}{4}\right]$$

5d gauge field A_μ $\Longrightarrow$ Conserved baryon charge $U(1)_B$

Dilaton-Maxwell coupling $f(\phi)$

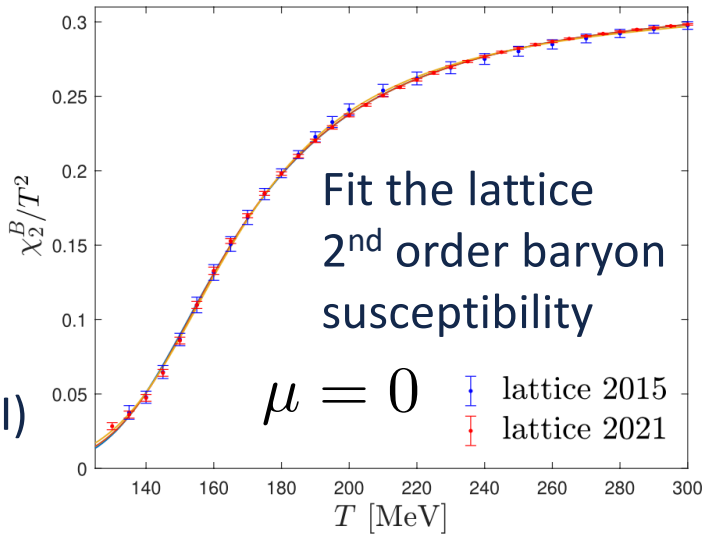

Backreaction from quark flavor branes (approx. of DBI) (describes chirally symmetric phase)

High-order baryon susceptibilities

Critelli et al, PRD (2017)

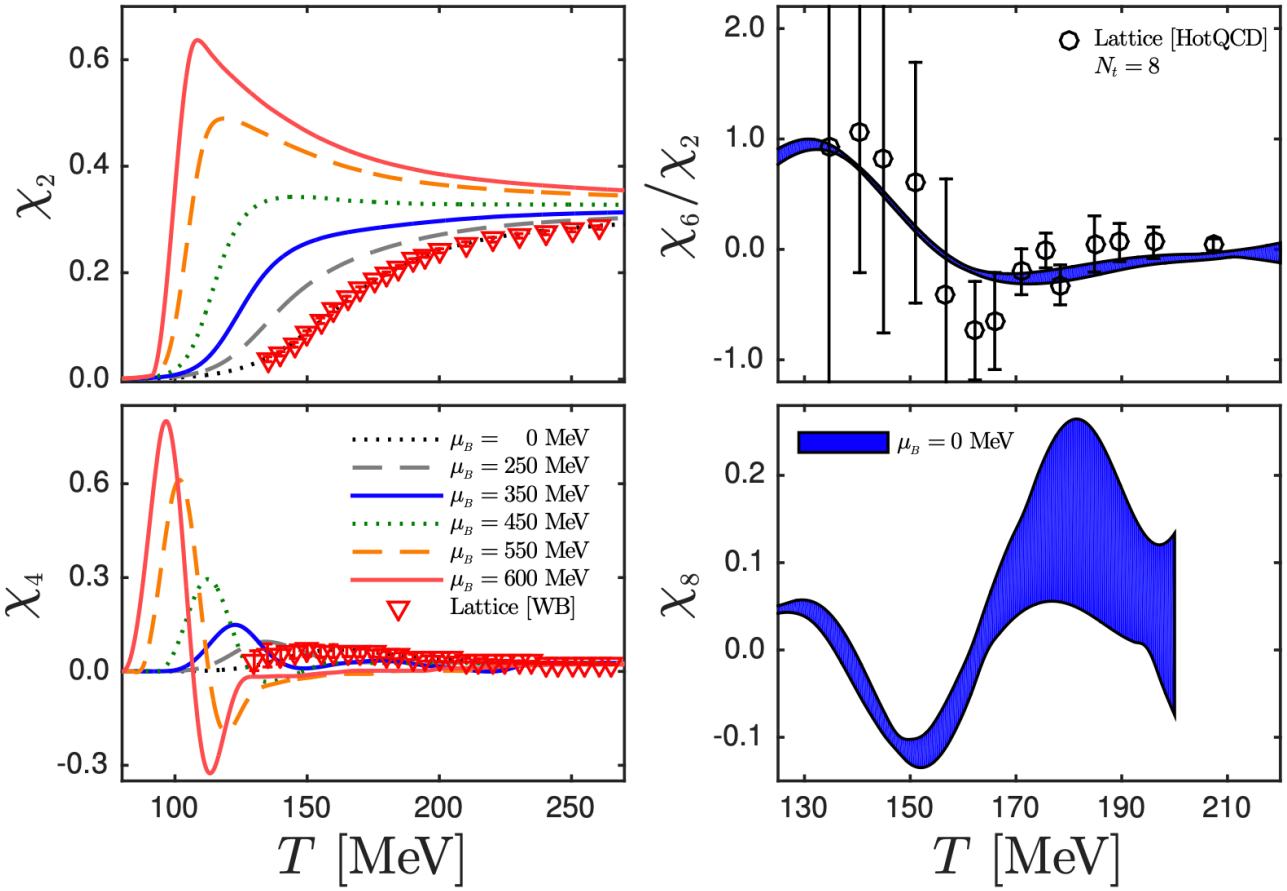

- Prediction for chi8 in 2017 compatible with lattice results (though not continuum extrapolated by then).

Critelli et al, PRD (2017)

Lattice: Borsányi et al, JHEP (2018)

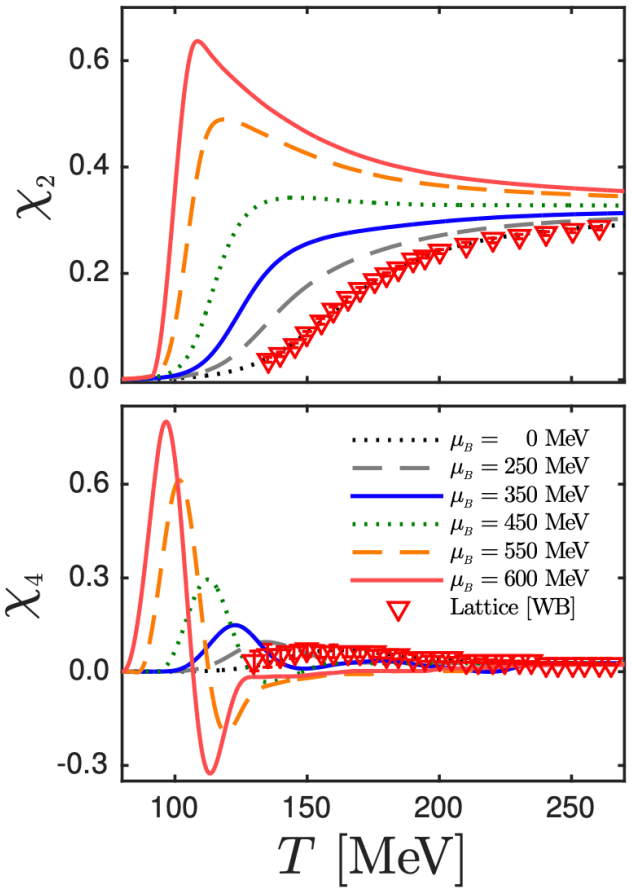

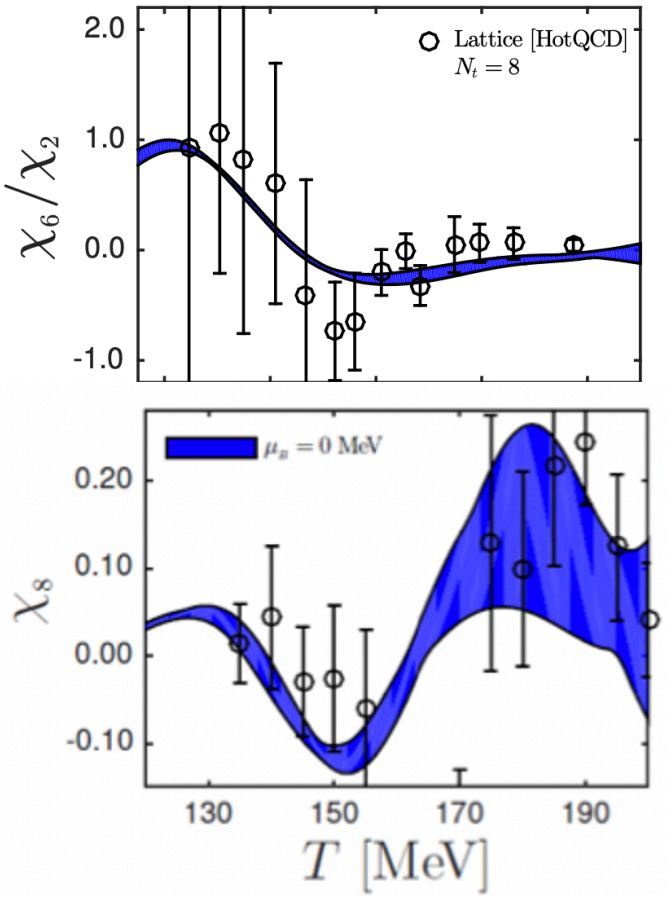

Ratio between baryon susceptibilities

Critelli et al, PRD (2017)

The shape and monotonicity properties depend on the path in the phase diagram: seeing a peak is important!

Mroczek et al, PRC (2021)

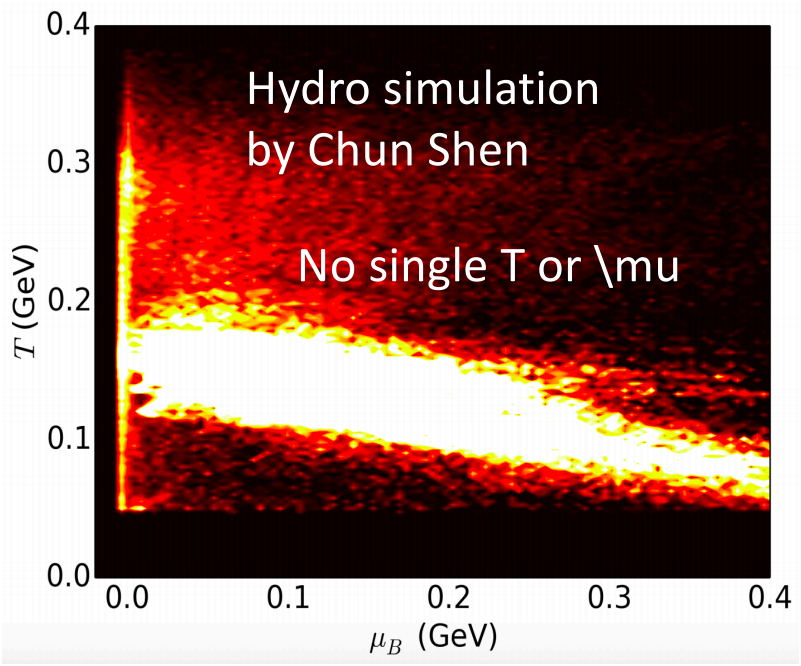

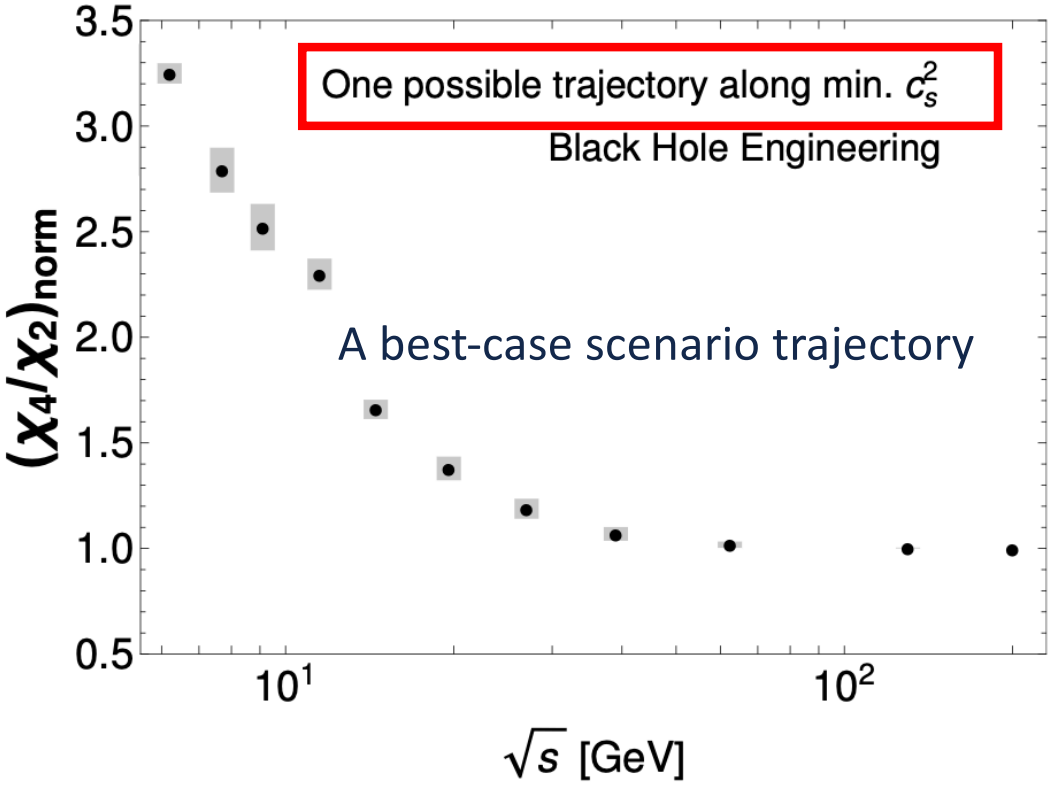

Finite density properties

Grefa et al, Phys. Rev. D 104, 034002 (2021)
Grefa et al, Phys. Rev. D 106 (2022) 034024

e-Print: 2309.00579 [nucl-th]

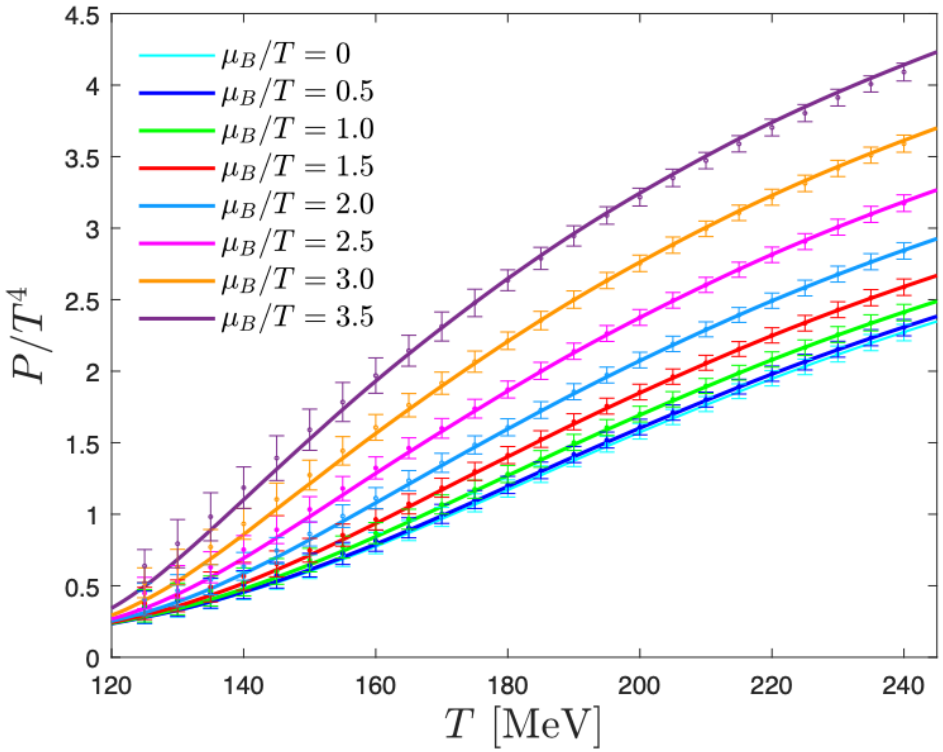

Lattice: Borsányi et al, PRL 126 (2021)

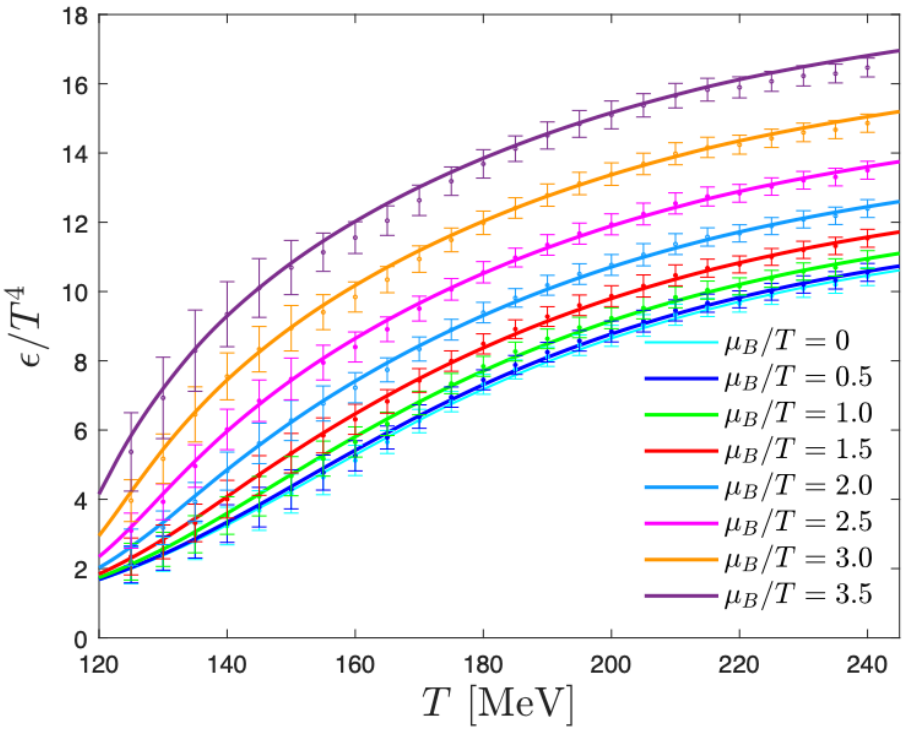

- Powerful, predictive model for baryon-rich QGP
- Real-time calculations (e.g. transport, hydro) possible

Precise determination of phase diagram

e-Print: 2309.00579 [nucl-th]

- Dilaton and electric fields at horizon: ϕ_0 and Φ_1 fully specify the physical state.
- Lines of constant ϕ_0 can cross.
- Metastable states, spinodal lines.
- Critical point: where crossings start.
  Fast algorithm to find CP!
- Maxwell construction: first-order line.

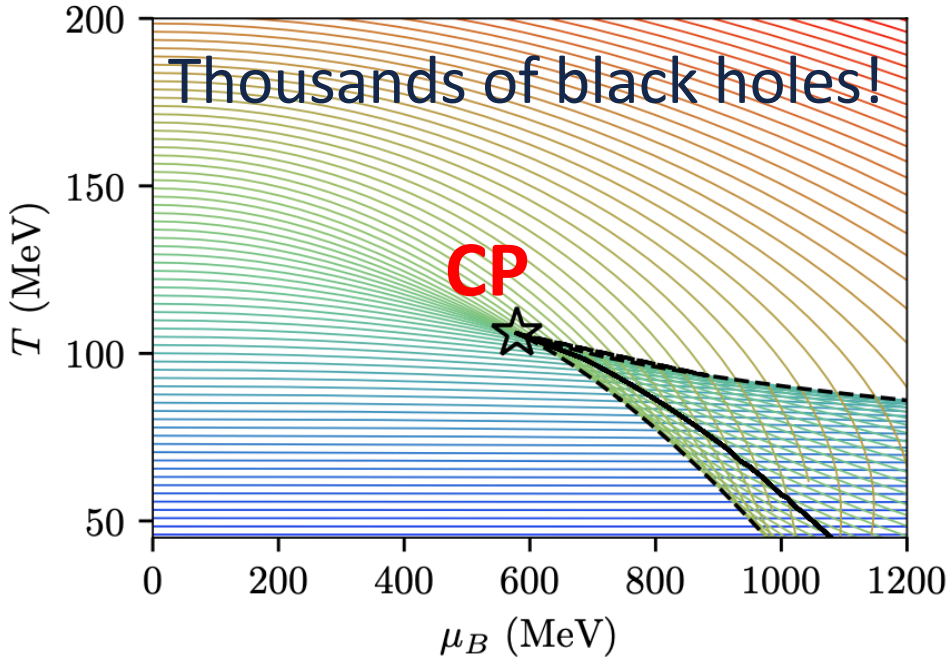

Fast and precise new algorithm = ripe for statistical analysis!

How do the many parameters affect CP?

Polynomial-Hyperbolic Ansatz (PHA)

e-Print: 2309.00579 [nucl-th]

- Interpolates between Phys. Rev. D 96 (2017) and Phys. Rev. D 104 (2021)

$$V(\phi) = -12\cosh(\gamma\,\phi) + b_2\,\phi^2 + b_4\,\phi^4 + b_6\,\phi^6$$

$$f(\phi) = \frac{\mathrm{sech}(c_1\phi + c_2\phi^2 + c_3\phi^3)}{1+d_1} + \frac{d_1}{1+d_1}\,\mathrm{sech}(d_2\phi)$$

Parametric Ansatz (PA)

- Similar shapes, more interpretable parameters Phys. Rev. D 96 (2017)

$$V(\phi) = -12\cosh\left[\left(\frac{\gamma_1\,\Delta\phi_V^2 + \gamma_2\,\phi^2}{\Delta\phi_V^2 + \phi^2}\right)\phi\right]$$

$$f(\phi) = 1 - (1-A_1)\left[\frac{1}{2} + \frac{1}{2}\tanh\left(\frac{\phi-\phi_1}{\delta\phi_1}\right)\right] - A_1\left[\frac{1}{2} + \frac{1}{2}\tanh\left(\frac{\phi-\phi_2}{\delta\phi_2}\right)\right]$$

Bayesian black hole engineering

e-Print: 2309.00579 [nucl-th]

- How do the many model parameters determine CP?
- Are CPs always present?
- How do lattice results + error bars affect CP location?
- Bayesian inference analysis needed!

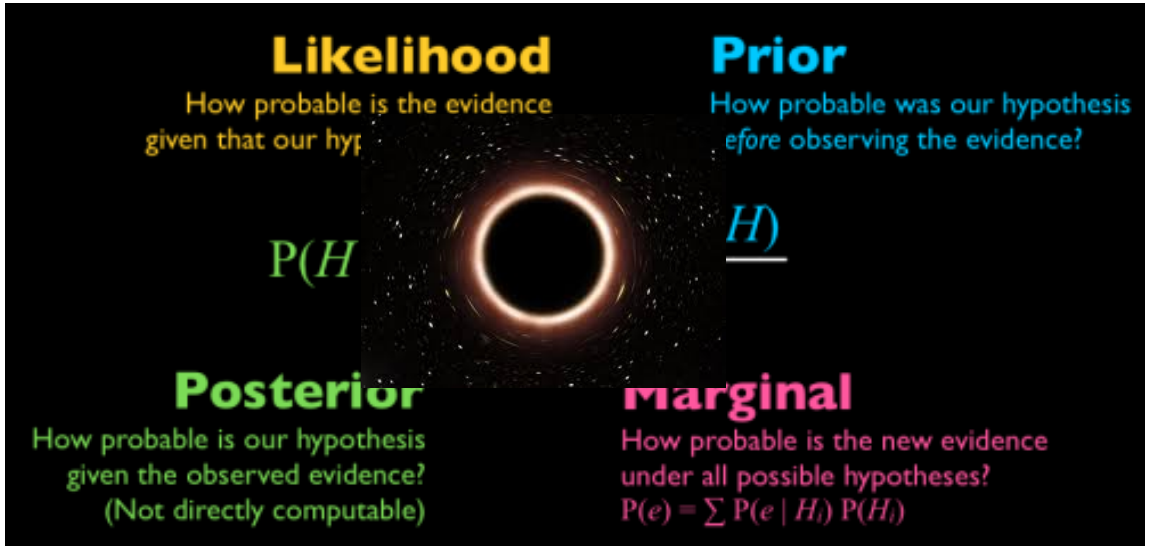

Bayesian black hole engineering

e-Print: 2309.00579 [nucl-th]

Assigning probabilities

Bayes' Theorem

$$\underbrace{P(\text{model}\,|\,\text{results})}_{\text{posterior } \mathcal{P}} \times P(\text{results}) = \underbrace{P(\text{results}\,|\,\text{model})}_{\text{likelihood } \mathcal{L}} \times \underbrace{P(\text{model})}_{\text{prior knowledge}}$$

Gaussian Likelihood

$$\mathcal{L} = \exp\left\{-\frac{1}{2}\boldsymbol{\delta x}^T \boldsymbol{\Sigma}^{-1} \boldsymbol{\delta x} - \frac{1}{2}\log\det\boldsymbol{\Sigma} + \text{constant}\right\}$$

- $\boldsymbol{\delta x}$: deviation for $s(T)$ and $\chi_2^{(B)}(T)$ at $\mu = 0$.
- Correlation $\Gamma \equiv \exp\left(-\Delta T/\xi_T\right)$ between neighboring points $\rightarrow$ extra model parameter.

Bayesian black hole engineering

e-Print: 2309.00579 [nucl-th]

Mauricio Hippert

Markov Chain Monte-Carlo (MCMC)

- Random evolution to sample from posterior.
- Transition probabilities such that $\mathcal{P}$ is stationary limit.
- Differential evolution MCMC: suited for correlations.

C.J.F. Ter Braak, Statistics and Computing **16** (2006)

Differential evolution

1. Use other chains j, k to update chain $i \neq j \neq k$: $\theta_i \to \theta_i + \frac{b}{\sqrt{2d}}(\theta_j - \theta_k) + \xi_i$.
2. Compute $\mathcal{P}$ from model EoS.
   - If $\mathcal{P}/\mathcal{P}_0 > 1$, transition to new parameters.
   - Otherwise, accept transition with probability $\mathcal{P}/\mathcal{P}_0$.
3. Repeat.

Inputs: Baryon susceptibility and entropy density from the lattice.

S. Borsanyi, Z. Fodor, C. Hoelbling, S. D. Katz, S. Krieg and K. K. Szabo, PRL **730** (2014)
Borsányi, Fodor, Guenther et al., PRL **126** (2021)

Bayesian black hole engineering

e-Print: 2309.00579 [nucl-th]

- **Flat prior for parameters**
- **20% of prior samples give no CP**

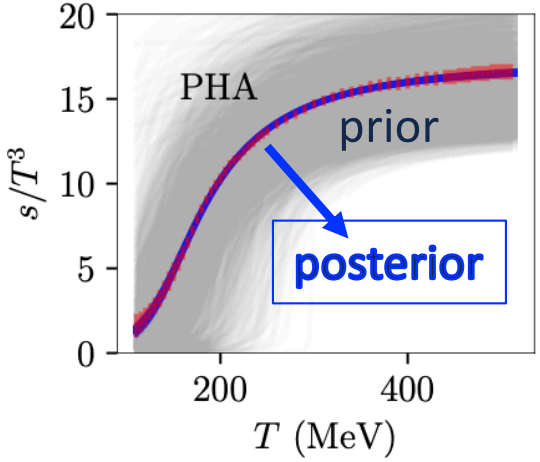

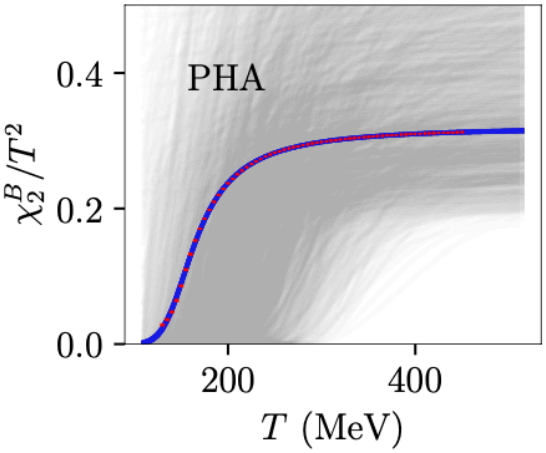

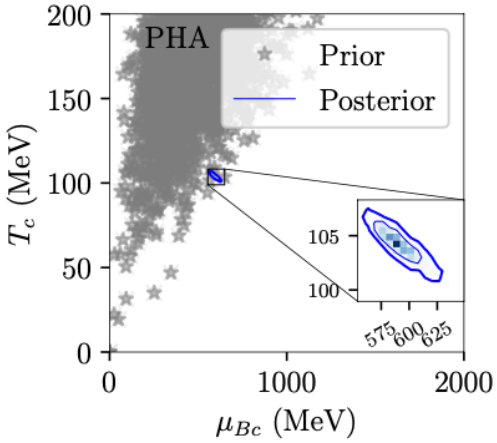

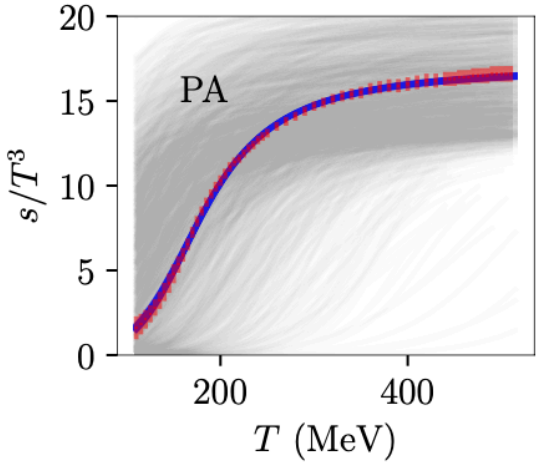

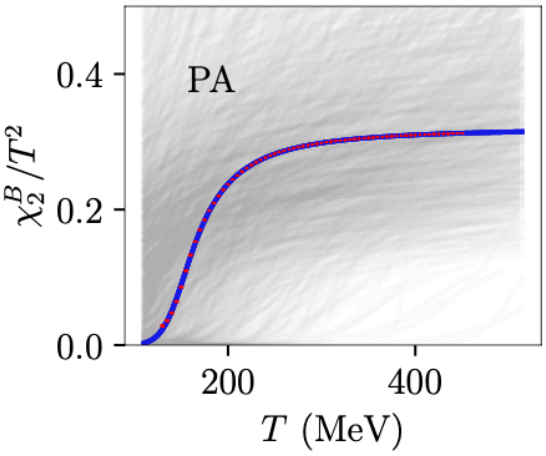

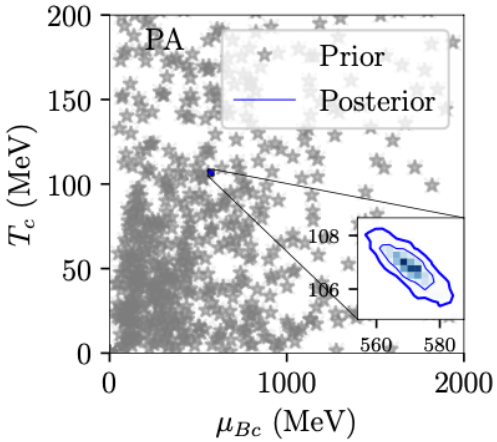

Bayesian inference in HIC 10 years ago …

Pratt, Sangaline, Sorensen, Wang, PRL (2015)

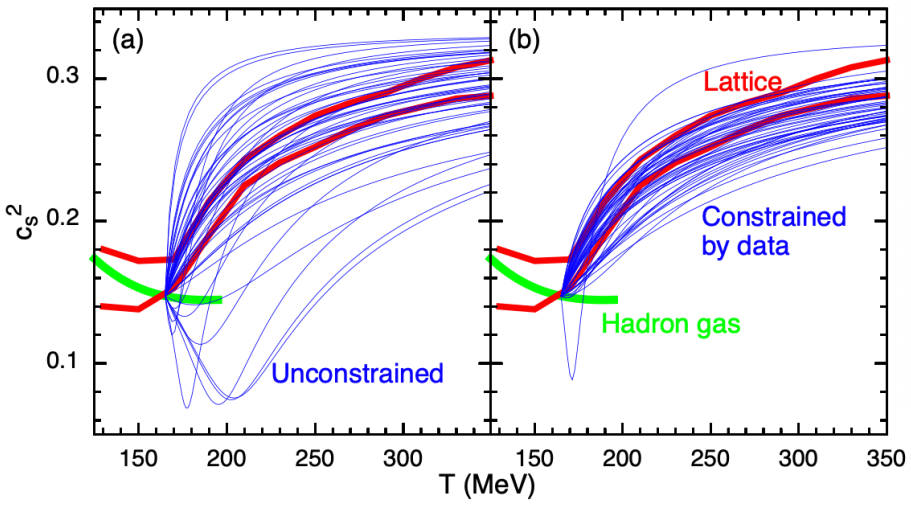

FIG. 5. (a) Fifty equations of state were generated by randomly choosing X' and R in Eq. (2) from the prior distribution and weighted by the posterior likelihood (b). The two upper thick lines in each figure represent the range of lattice equations of state shown in [4], and the lower thick line shows the equation of state of a non-interacting hadron gas. This suggests that the matter created in heavy-ion collisions at RHIC and at the LHC has a pressure that is similar, or slightly softer, to that expected from equilibrated matter.

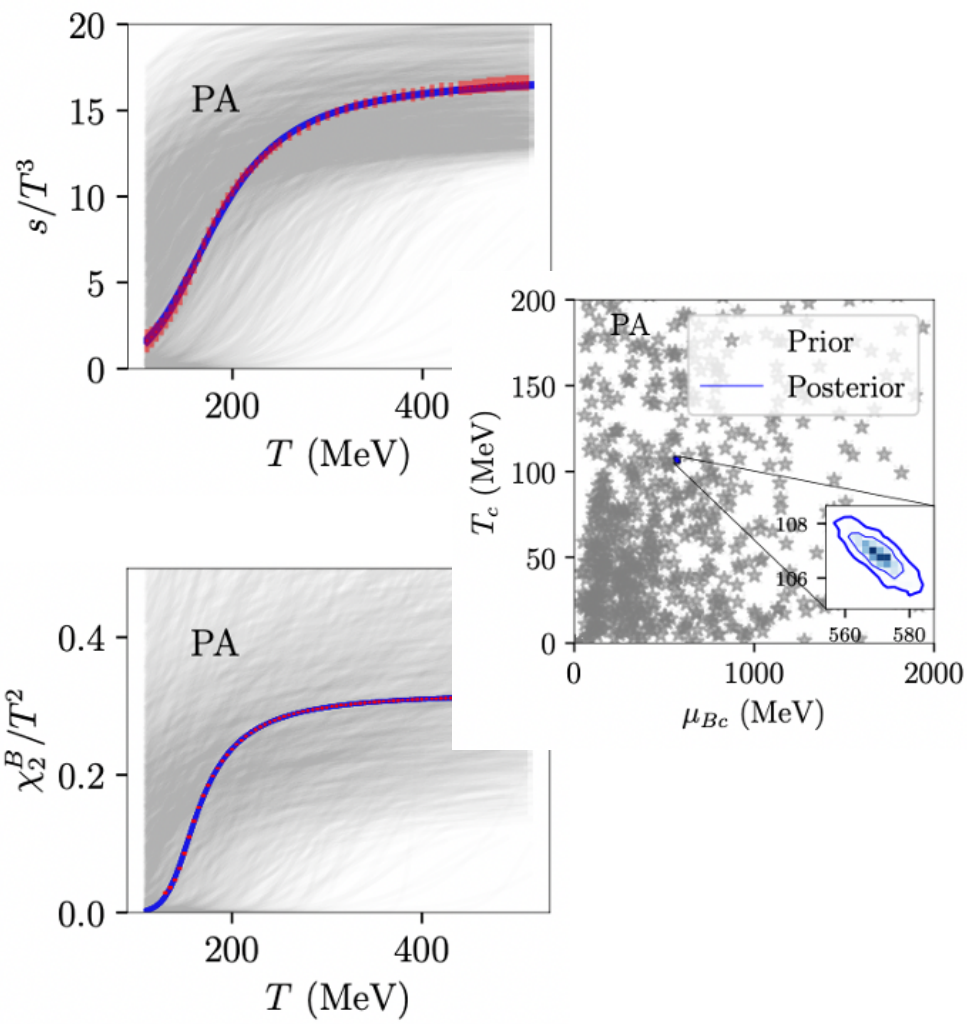

Prior distributions

FLAT PRIOR

e-Print: 2309.00579 [nucl-th]

PHA Ansatz		
Parameter	min	max
Λ	800 MeV	1400 MeV
κ_2	9.0	15.0
γ	0.5682	0.6500
b_2	-0.05	0.65
b_4	-0.150	-0.015
b_6	-0.00200	0.00169
c_1	-0.035	0.100
c_2	0.1	1.5
c_3	0.0	1.0
d_1	0.0	2.5
d_2 (J)	3	10000

PA Ansatz		
Parameter	min	max
Λ	400 MeV	1400 MeV
κ_2	9.0	15.0
γ_1	0.40	0.57
γ_2	0.50	0.68
$\Delta\phi_V$	1.5	3.0
A	0.25	0.50
ϕ_1	-0.1	0.5
$\delta\phi_1$ (J)	10^{-5}	0.3
ϕ_2	0.8	4.5
$\delta\phi_2$	0.2	4.0

TABLE I. Prior ranges for parameters in the PHA (left) and PA (right) models. The '(J)' marks parameters for which we have used *Jeffreys* priors — i.e., prior distributions that are uniform over the logarithm of these parameters.

Posterior distributions

e-Print: 2309.00579 [nucl-th]

PHA	Posterior 95% CI		
Parameter	min	max	MAP
Λ	1089 MeV	1190 MeV	1129 MeV
κ_2	11.3	11.5	11.4
γ	0.57	0.63	0.58
b_2	0.1	0.5	0.2
b_4	-0.06	-0.03	-0.05
b_6	0.000	0.002	0.0007
c_1	-0.1	0.1	0.0
c_2	0.1	0.3	0.2
c_3	0.01	0.08	0.04
d_1	1.70	1.74	1.72
d_2 (J)	113	8068	1294

PA	Posterior 95% CI		
Parameter	min	max	MAP
Λ	862 MeV	1043 MeV	955 MeV
κ_2	11.3	11.5	11.4
γ_1	0.50	0.54	0.52
γ_2	0.60	0.62	0.61
$\Delta\phi_V$	1.6	2.1	1.8
A	0.369	0.374	0.371
ϕ_1	0.000	0.025	0.002
$\delta\phi_1$ (J)	0.0001	0.0032	0.0003
ϕ_2	2.1	2.3	2.2
$\delta\phi_2$	0.65	0.73	0.69

TABLE II. Posterior 95% confidence intervals (95% CI) and maximum a posteriori (MAP) values for parameters of the PHA (left) and PA (right) models. The '(J)' marks parameters for which we have used *Jeffreys* priors — i.e., prior distributions that are uniform over the logarithm of these parameters. MAP values are extracted by maximizing the likelihood.

PHA

e-Print: 2309.00579 [nucl-th]

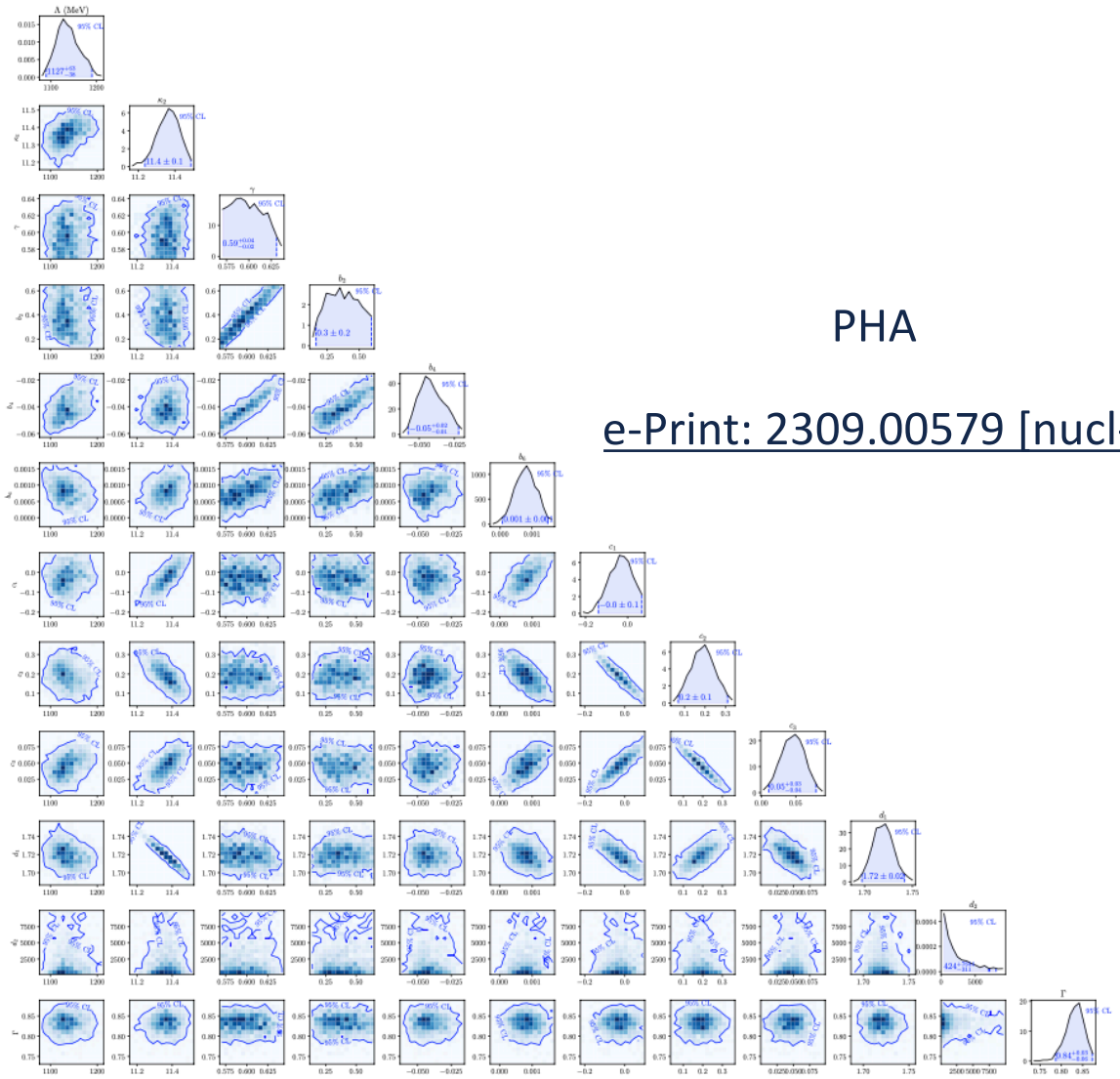

FIG. 5. Marginalized a posteriori probability distributions for pairs of parameters of the PHA model. Solid lines show 95% confidence intervals. On the diagonal, marginalized one-parameter posterior distributions are also shown, along with the marginalized maximum a posteriori (MMAP) value and 95% confidence interval for each parameter. MMAP values are extracted by maximizing the marginalized one-parameter posterior distributions.

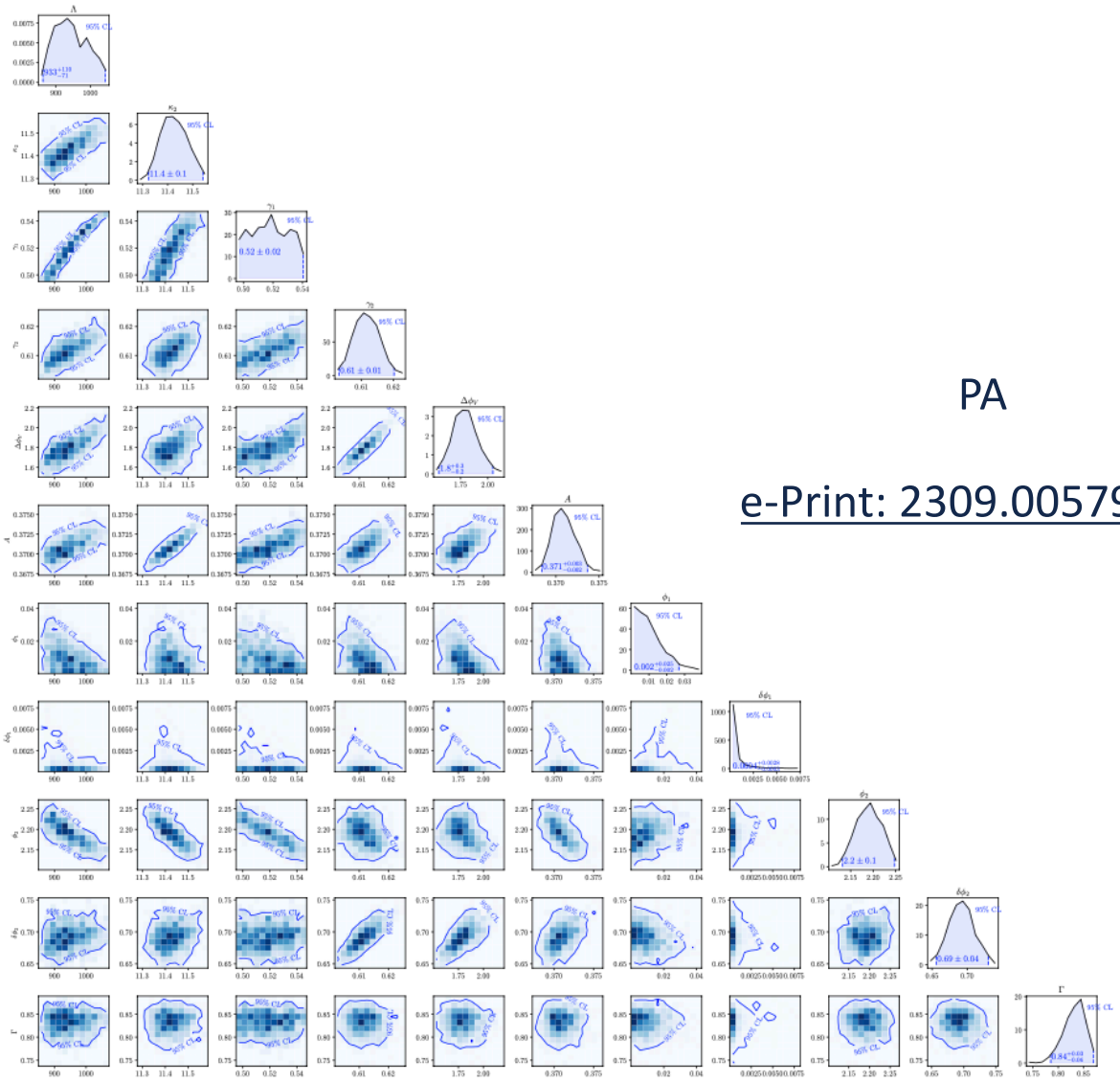

FIG. 6. Marginalized a posteriori probability distributions for pairs of parameters of the PA model. Solid lines show 95% confidence intervals. On the diagonal, marginalized one-parameter posterior distributions are also shown, along with the marginalized maximum a posteriori (MMAP) value and 95% confidence interval for each parameter. MMAP values are extracted by maximizing the marginalized one-parameter posterior distributions.

PA

e-Print: 2309.00579 [nucl-th]

LIKELIHOOD FUNCTION

The agreement between predictions $\vec{p}(\theta)$ of the model with parameters θ and lattice QCD results $\vec{d}$ is quantified by the likelihood function $\mathcal{L}(\vec{\theta}) \equiv P(\vec{d}|\vec{\theta})$.

We take a Gaussian likelihood

$$\mathcal{L}(\vec{\theta}) = \frac{1}{\prod\limits_{Q=s,\chi_2}\left[\left(\prod\limits_i \sigma_i^{(Q)}\right)\sqrt{2\pi\det\Lambda}\right]} \exp\left\{-\frac{1}{2}\sum_{i,j}\sum_{Q=s,\chi_2}\frac{p_i^{(Q)}(\vec{\theta})-d_i^{(Q)}}{\sigma_i^{(Q)}}\left[\Lambda^{-1}\right]_{ij}\frac{p_j^{(Q)}(\vec{\theta})-d_j^{(Q)}}{\sigma_j^{(Q)}}\right\}, \tag{S.1}$$

where $\sigma_i^{(Q)}$, with $Q = s, \chi_2^B$ represent error bars for the different points from lattice QCD.

$$\log\mathcal{L} = \frac{-1}{1-\Gamma^2}\left[(1+\Gamma^2)\,\zeta^2 - \Gamma\,\psi - \Gamma^2\,\phi\right] - (N-1)\,\log(1-\Gamma^2) + \text{const.},$$

$$\zeta^2 \equiv \frac{1}{2}\sum_i\sum_{Q=s,\chi_2}\left(\frac{p_i^{(Q)}(\vec{\theta})-d_i^{(Q)}}{\sigma_i^{(Q)}}\right)^2,$$

$$\psi \equiv \sum_i\sum_{Q=s,\chi_2}\frac{p_i^{(Q)}(\vec{\theta})-d_i^{(Q)}}{\sigma_i^{(Q)}}\frac{p_{i+1}^{(Q)}(\vec{\theta})-d_{i+1}^{(Q)}}{\sigma_{i+1}^{(Q)}},$$

$$\phi \equiv \frac{1}{2}\left[\left(\frac{p_1^{(Q)}(\vec{\theta})-d_1^{(Q)}}{\sigma_1^{(Q)}}\right)^2 + \left(\frac{p_N^{(Q)}(\vec{\theta})-d_N^{(Q)}}{\sigma_N^{(Q)}}\right)^2\right].$$

Remarkably, the posterior 95% confidence interval obtained for the correlation strength is of $\Gamma = 0.84^{+0.03}_{-0.06}$, for both the PHA and PA models. This impressive agreement indicates that its value does not reflect the parametrization, but rather the lattice QCD error bars.

e-Print: 2309.00579 [nucl-th]

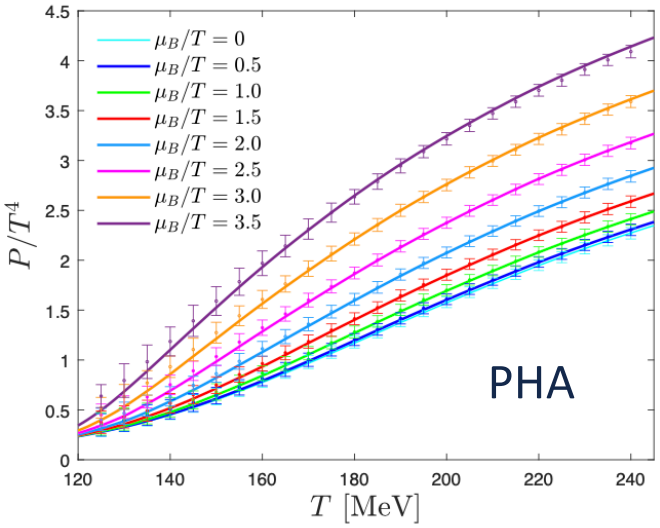

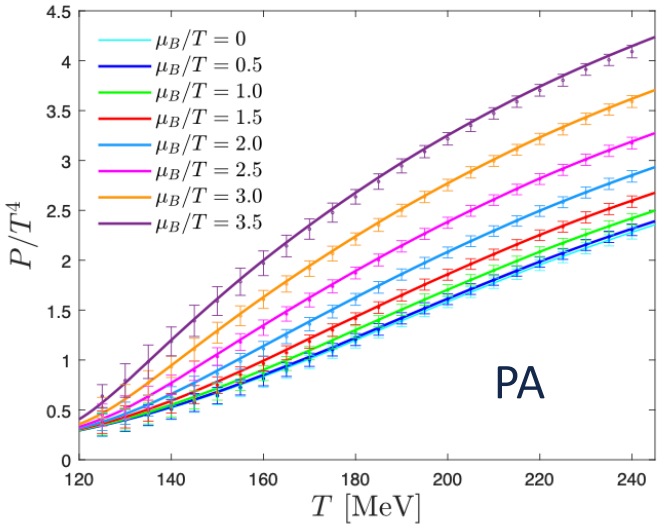

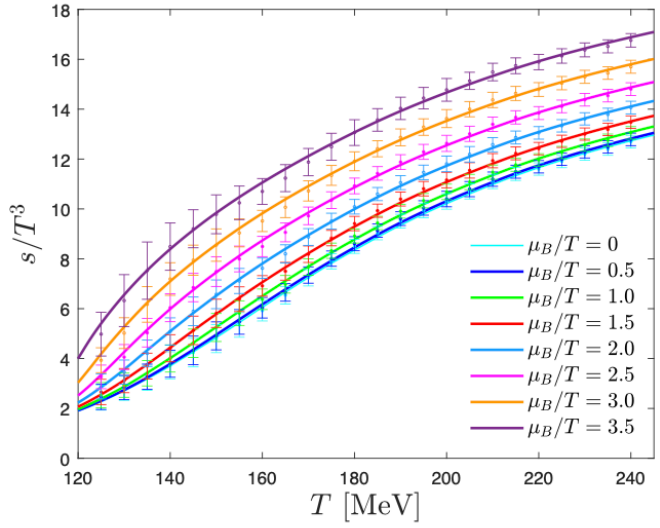

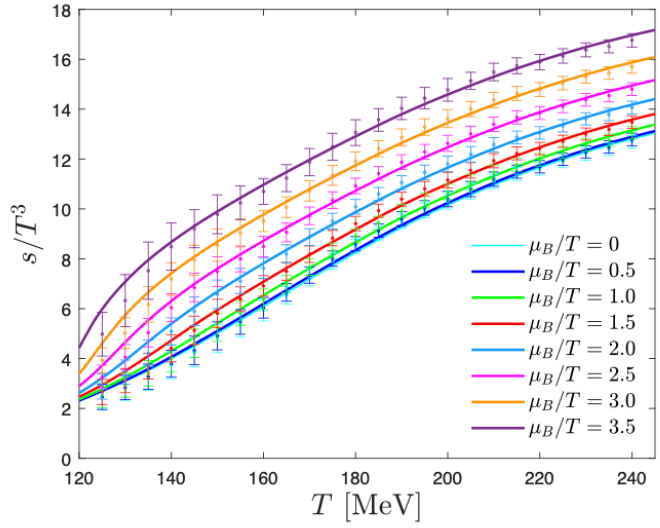

e-Print: 2309.00579 [nucl-th]

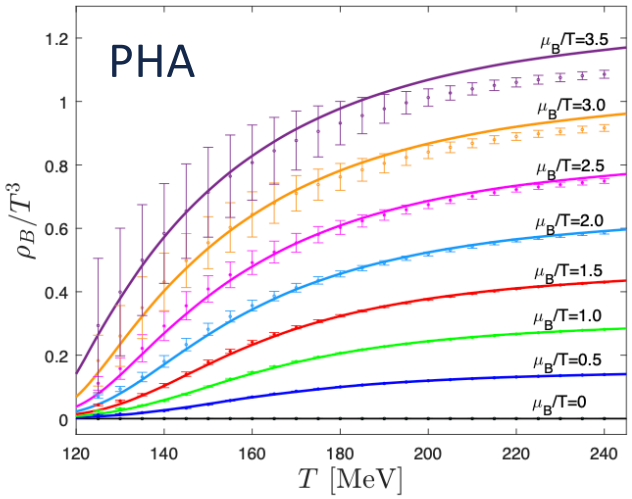

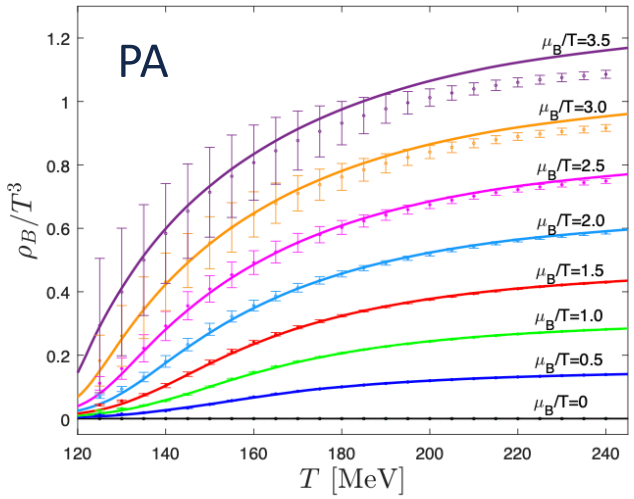

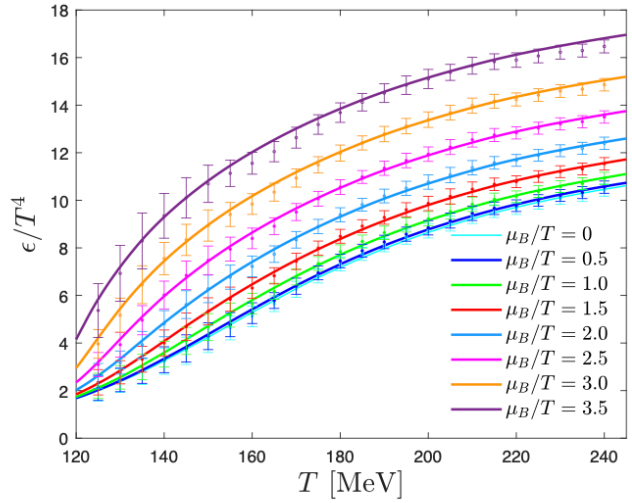

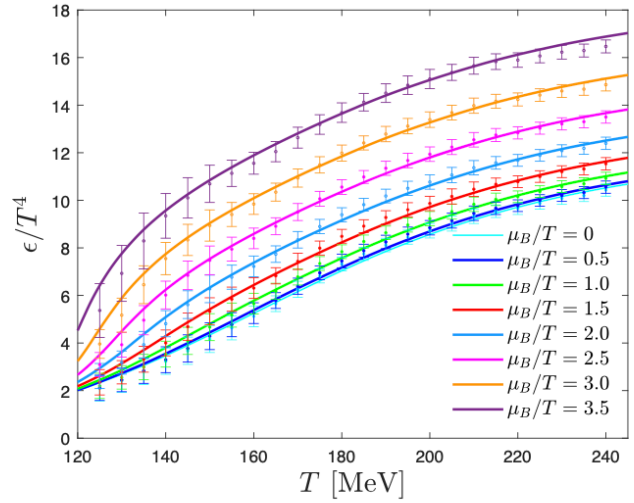

e-Print: 2309.00579 [nucl-th]

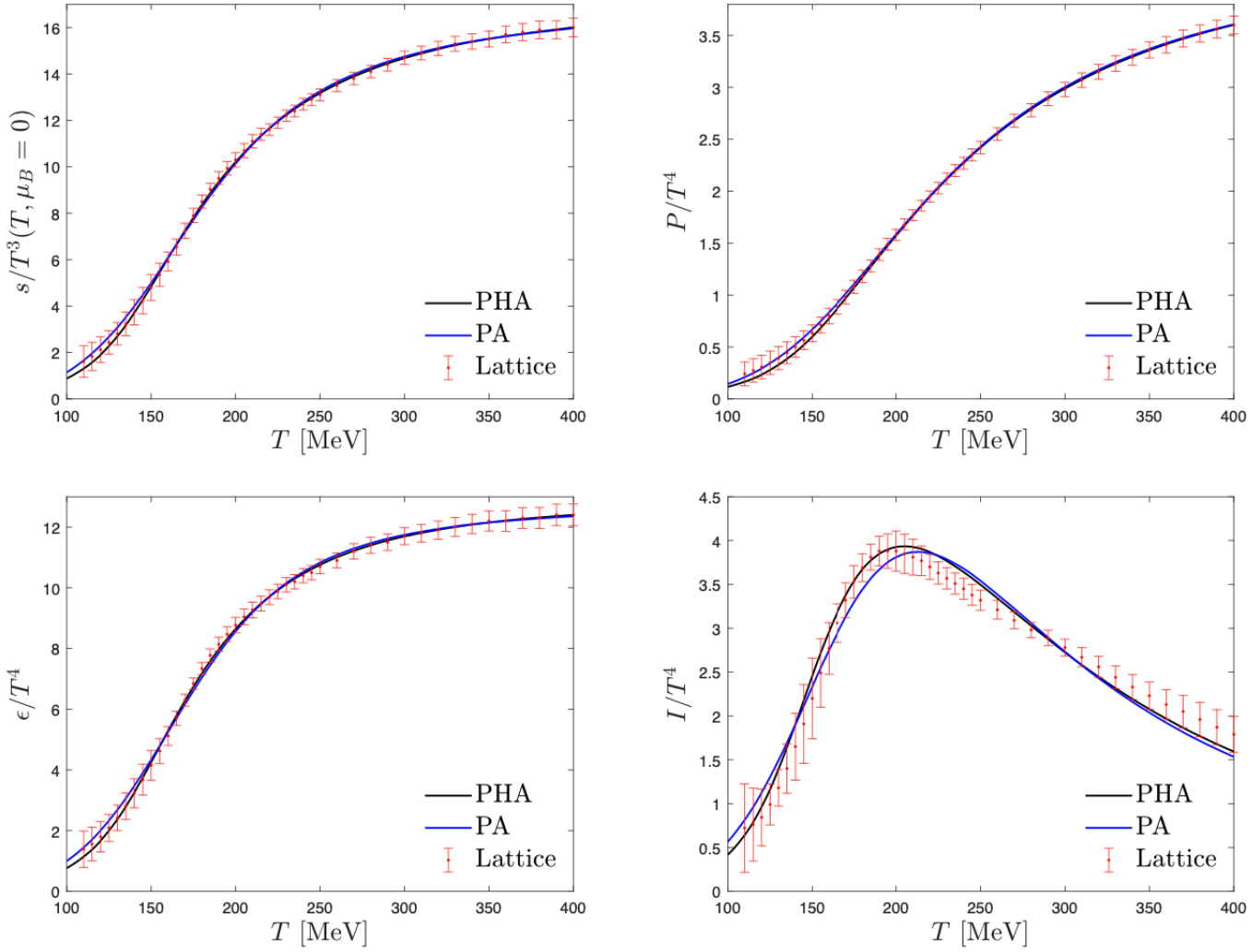

FIG. 8. Comparison between the best fit for the PHA and PA models and the lattice equation of state at zero chemical potential from Ref. [25]

Bayesian black hole engineering

e-Print: 2309.00579 [nucl-th]

All posterior predictions for CP location collapse around these regions

Posterior critical points

$(T_c,\ \mu_{Bc})_{PHA} = (104 \pm 3,\ 589^{+36}_{-26})$ MeV, $(T_c,\ \mu_{Bc})_{PA} = (107 \pm 1,\ 571 \pm 11)$ MeV.

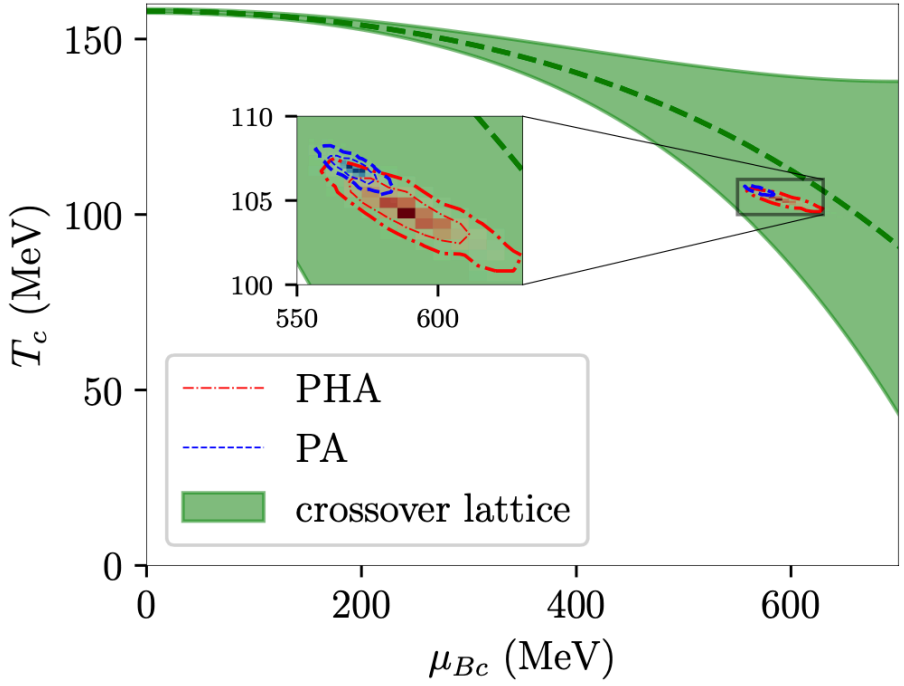

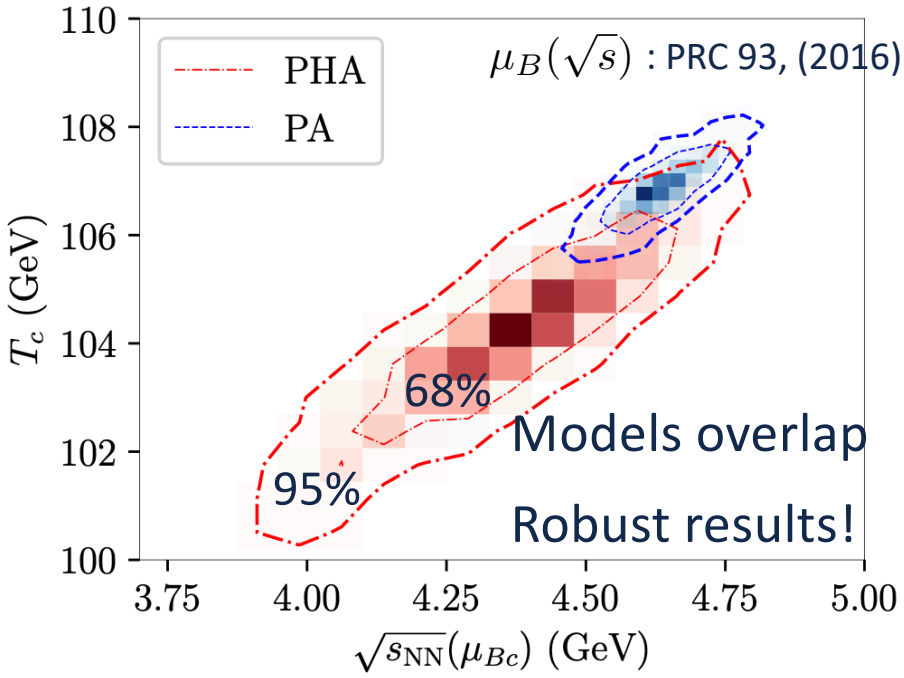

Location of CP from holography

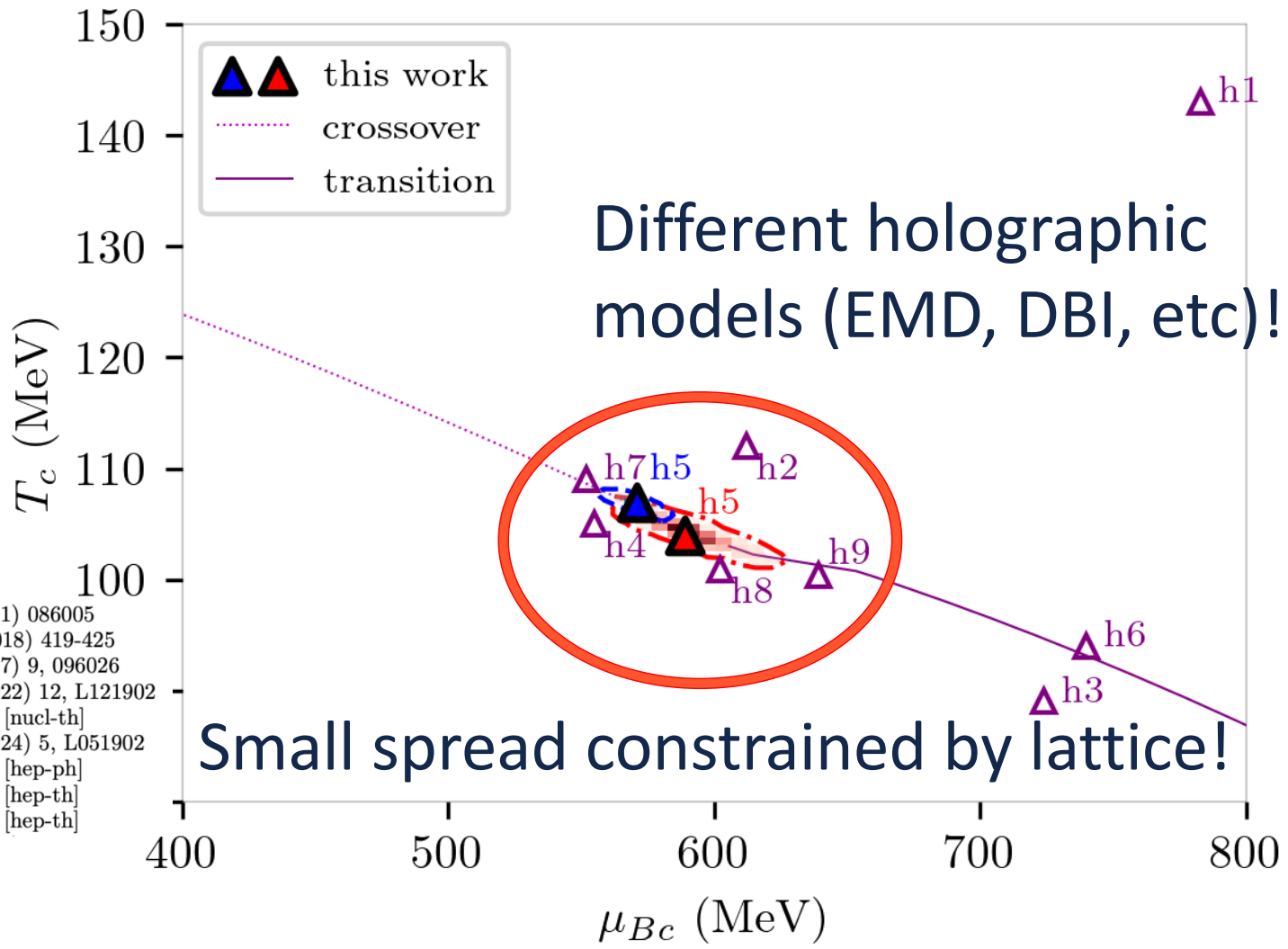

h1: Phys.Rev.D 83 (2011) 086005
h2: Phys.Lett.B 778 (2018) 419-425
h3: Phys.Rev.D 96 (2017) 9, 096026
h4: Phys.Rev.D 106 (2022) 12, L121902
h5: e-Print: 2309.00579 [nucl-th]
h6: Phys.Rev.D 109 (2024) 5, L051902
h7: e-Print: 2404.12109 [hep-ph]
h8: e-Print: 2405.02394 [hep-th]
h9: e-Print: 2405.02394 [hep-th]

Location of CP from holography

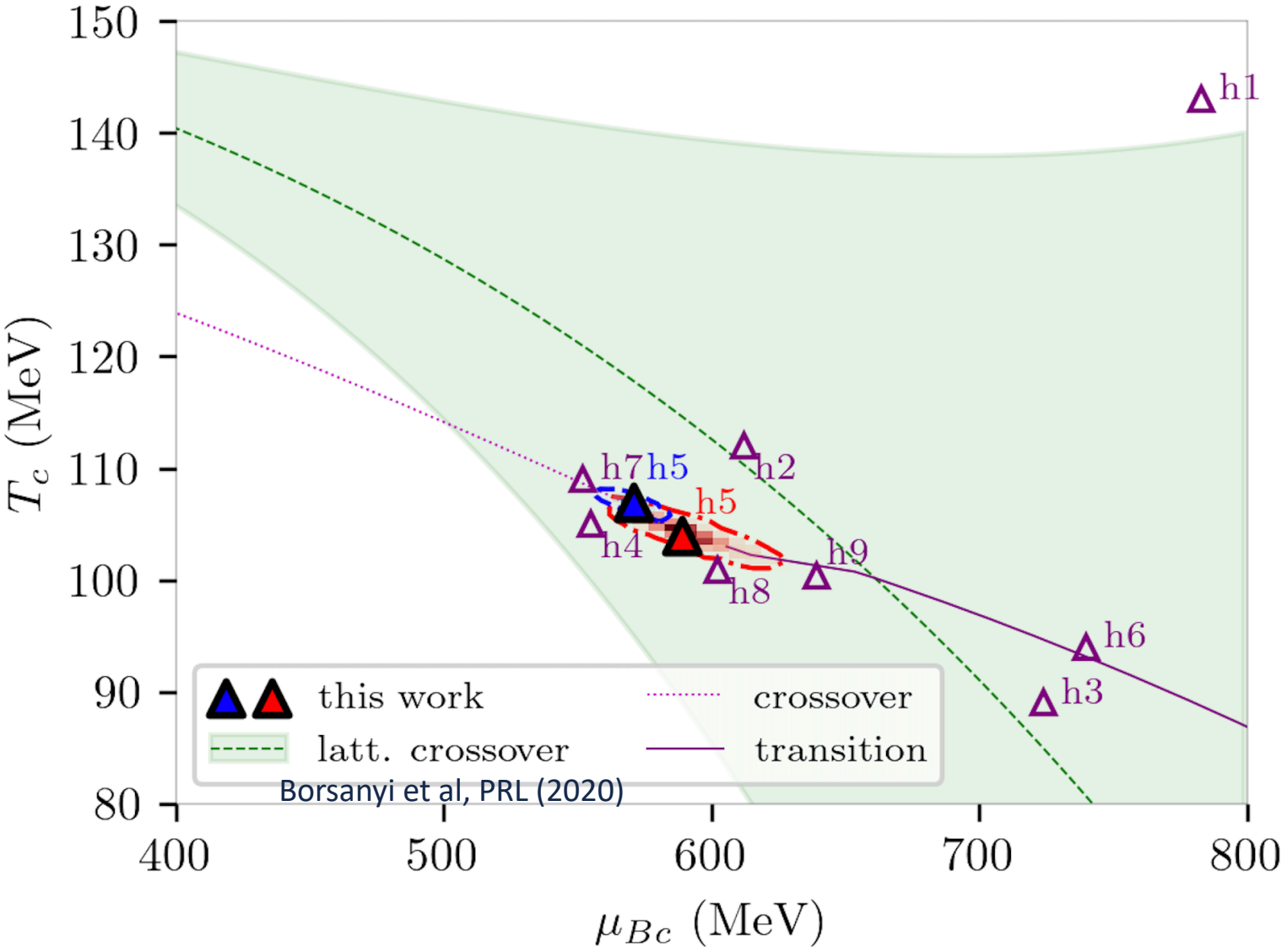

Location of CP from models: 18 years ago

M. Stephanov, Lattice 2006 Plenary talk, arXiv:hep-lat/0701002

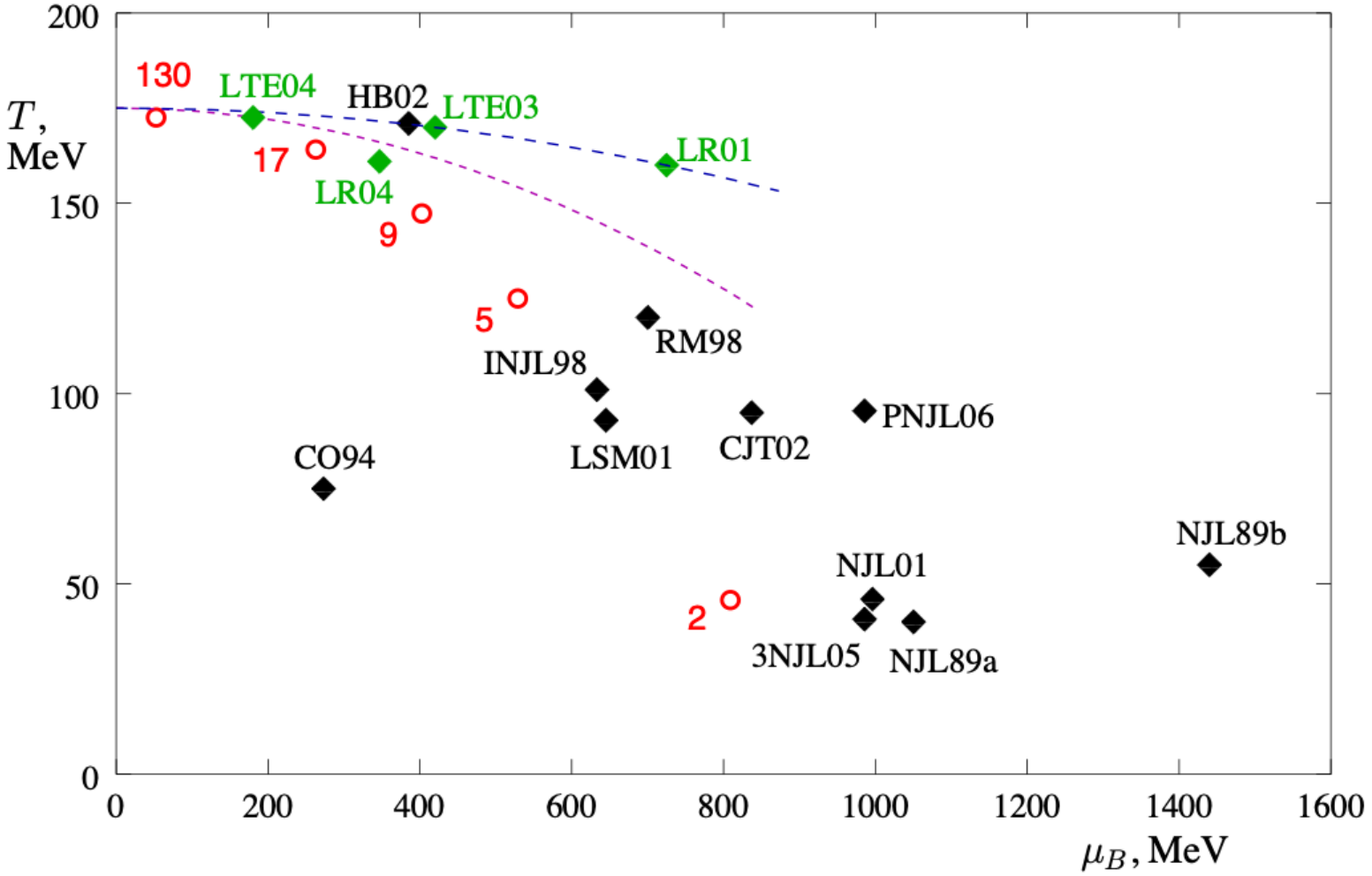

Location of CP from models: 18 years ago

M. Stephanov, Lattice 2006 Plenary talk, arXiv:hep-lat/0701002

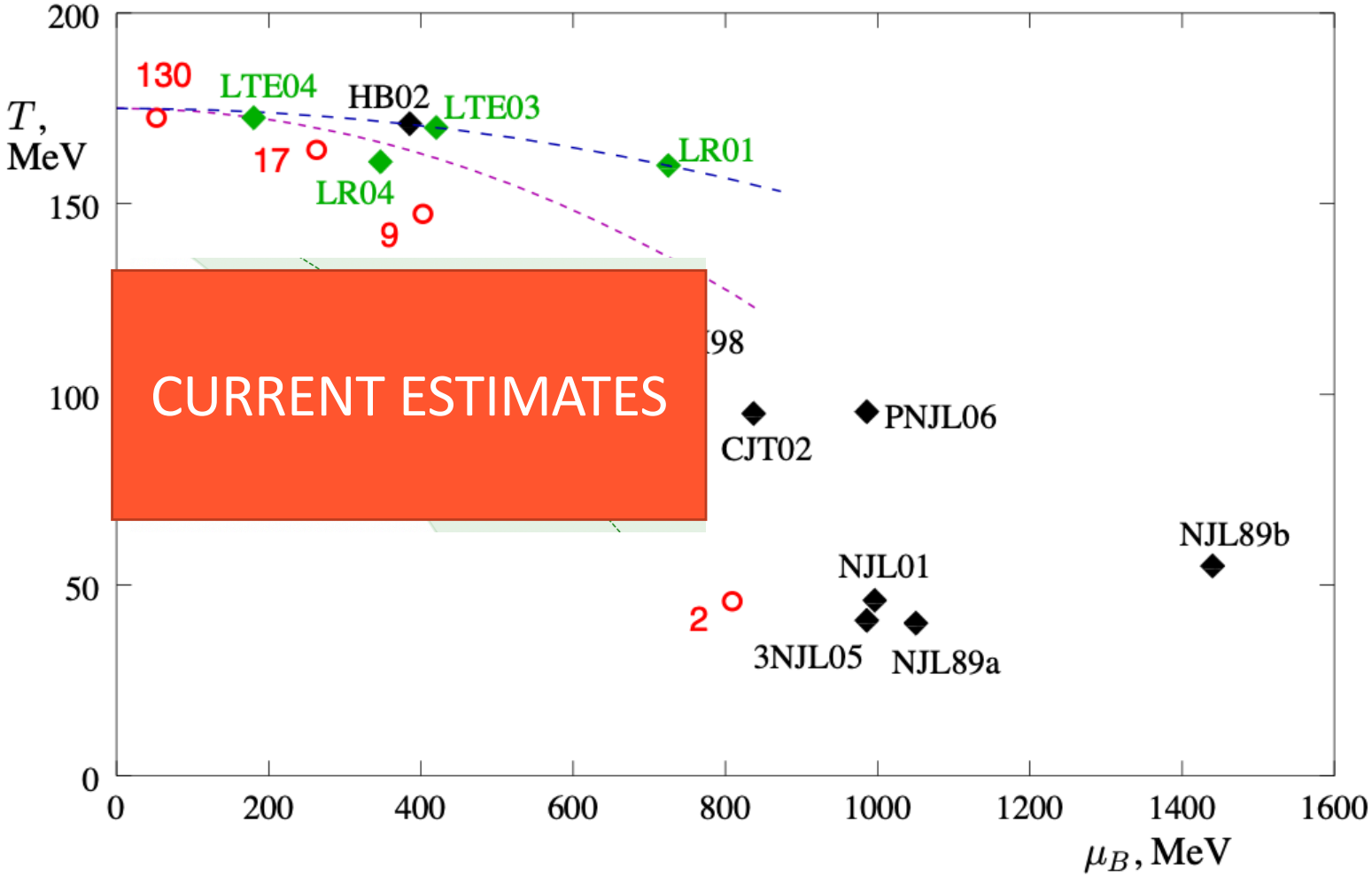

Location of CP from models: 18 years ago

M. Stephanov, Lattice 2006 Plenary talk, arXiv:hep-lat/0701002

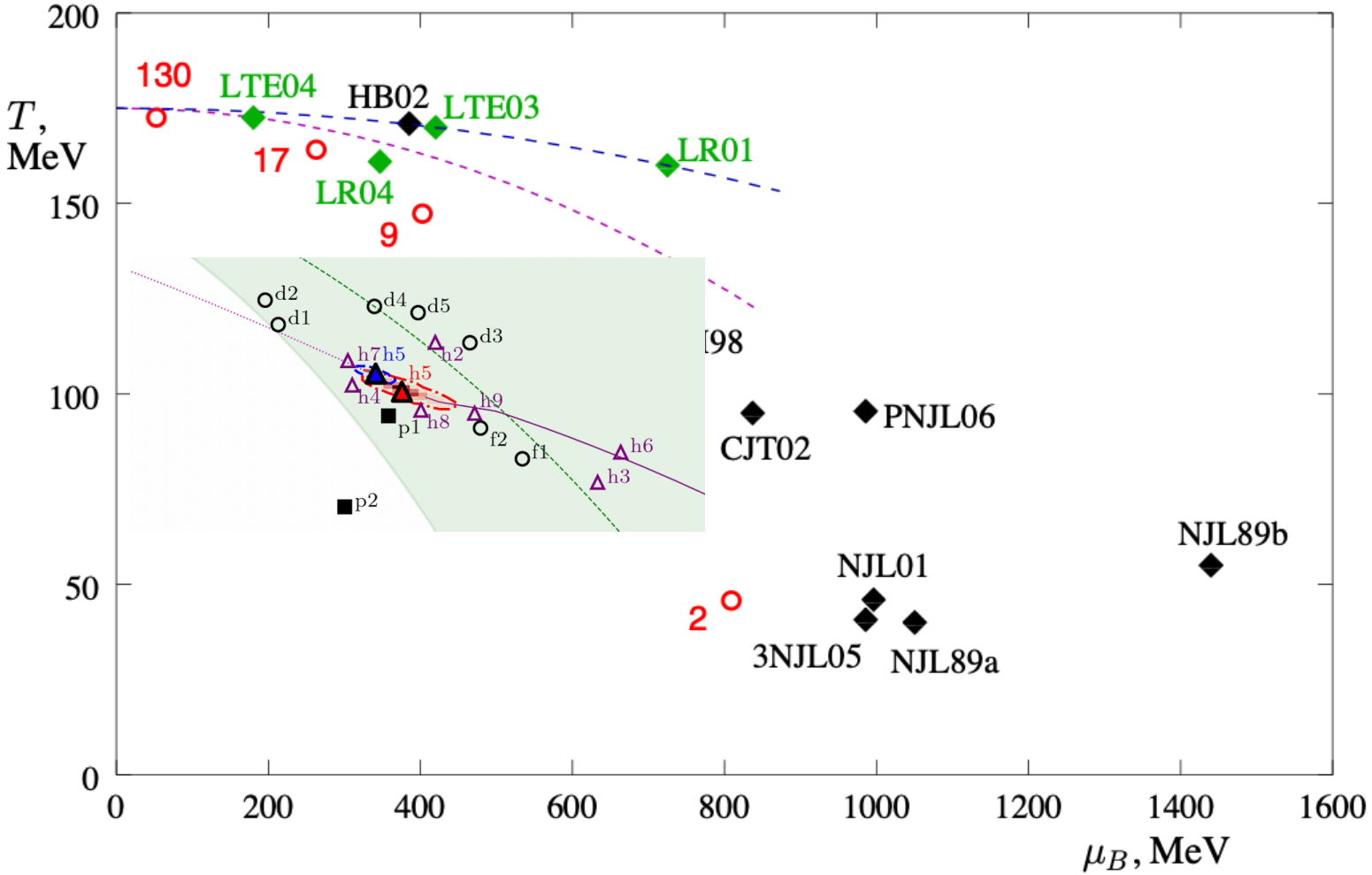

Current estimates for the CP location

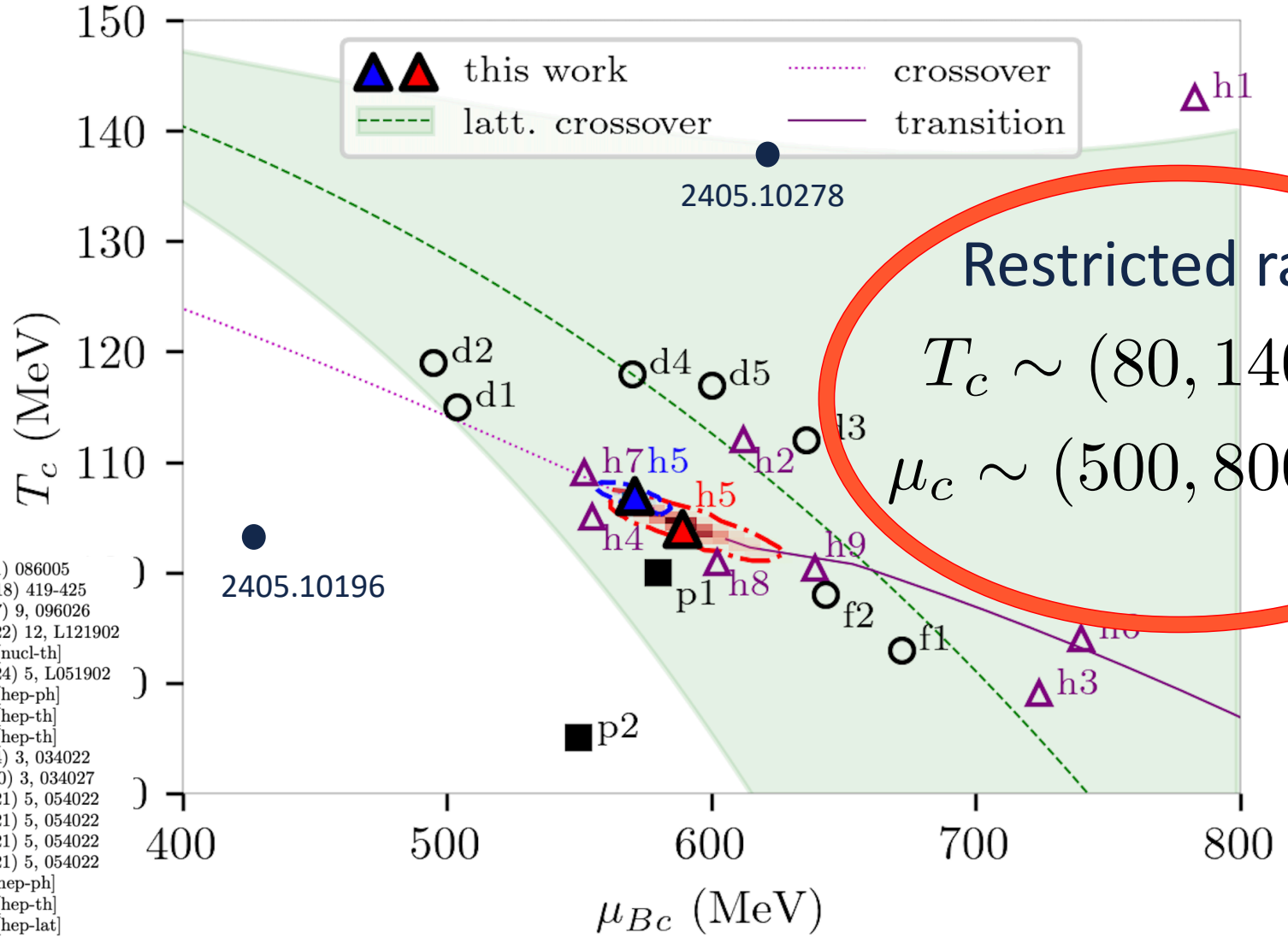

Restricted range

$T_c \sim (80, 140)$ MeV

$\mu_c \sim (500, 800)$ MeV

h1: Phys.Rev.D 83 (2011) 086005
h2: Phys.Lett.B 778 (2018) 419-425
h3: Phys.Rev.D 96 (2017) 9, 096026
h4: Phys.Rev.D 106 (2022) 12, L121902
h5: e-Print: 2309.00579 [nucl-th]
h6: Phys.Rev.D 109 (2024) 5, L051902
h7: e-Print: 2404.12109 [hep-ph]
h8: e-Print: 2405.02394 [hep-th]
h9: e-Print: 2405.02394 [hep-th]
d1: Phys.Rev.D 90 (2014) 3, 034022
f1: Phys.Rev.D 102 (2020) 3, 034027
d2: Phys.Rev.D 104 (2021) 5, 054022
d3: Phys.Rev.D 104 (2021) 5, 054022
d4: Phys.Rev.D 104 (2021) 5, 054022
d5: Phys.Rev.D 104 (2021) 5, 054022
f2: e-Print: 2308.15508 [hep-ph]
p1: e-Print: 2312.06952 [hep-th]
p2: e-Print: 2401.08820 [hep-lat]

Conclusions

• Location of QCD CP from a Bayesian analysis constrained by lattice results at zero net baryon density:

Predict CEP (95% confidence level):

$$T_c = 101 - 108 \text{ MeV}$$
$$\mu_c = 560 - 625 \text{ MeV}$$

$$\frac{\mu_c}{T_c} \sim 5 - 6$$

• Other approaches (FRG,DSE, FSS, Pade, etc) predict CP in a similar narrow range.

• Approaches didn't have to agree: *who ordered that?*